arXiv:hep-ph/9404202v1 1 Apr 1994

CLAN PROPERTIES IN PARTON SHOWERS

R. Ugoccioni,   A. Giovannini,   S. Lupia

Dipartimento di Fisica Teorica, Università di Torino
and INFN, Sezione di Torino
via P. Giuria 1, 10125 Torino, Italy

ABSTRACT

By considering clans as genuine elementary subprocesses, *i.e.*, intermediate parton sources in the Simplified Parton Shower model, a generalized version of this model is defined. It predicts analytically clan properties at parton level in agreement with the general trends observed experimentally at hadronic level and in Monte Carlo simulations both at partonic and hadronic level. In particular the model shows a linear rising in rapidity of the average number of clans at fixed energy of the initial parton and its subsequent bending for rapidity intervals at the border of phase space, and approximate energy independence of the average number of clans in fixed rapidity intervals. The energy independence becomes stricter by properly normalizing the average number of clans.

Introduction

Clan concept was introduced in [1] in order to interpret the wide occurrence of NB regularity in terms of a two step cascade process. Clans are defined, as well known, as group of particles of common ancestor; they are independently produced and each clan contains at least one particle. With these assumptions the average number of clans is distributed according to a Poisson distribution. Negative Binomial (NB) behavior is obtained by requiring in addition that particles inside an average clan have a logarithmic distribution which results from the convolution of truncated geometric distributions for particles within single clans[2].

Clan structure analysis in terms of the average number of clans, $\bar{N}$, and of the average number of particles per clan, $\bar{n}_c$, at final hadron level has given striking and unexpected results which are still puzzling. In particular it has been shown that the density of clans per unit of rapidity in symmetric rapidity intervals, although different in e^+e^- annihilation[3] from deep inelastic scattering[4] and hadron-hadron collisions[5], is approximately independent of the c.m. energy of the collision; furthermore the average number of clans at fixed c.m. energy grows initially linearly with the width of the rapidity interval, then a characteristic bending is seen at the border of phase space.

It should be pointed out that these regularities are satisfied with a higher degree of accuracy at final parton level than at final hadron level as it was seen by applying clan structure analysis to the final parton Multiplicity Distributions (MD's) in symmetric rapidity intervals reconstructed *via* Generalized Local Parton Hadron Duality (GLPHD) hadronization prescription[6] from the corresponding MD's at final hadron level[7]. The conclusion was that a complex phenomenon like Multiparticle Production might very well be at parton level more elementary than at final hadron level.

The natural question at this point was the following: is simplicity maintained at an even more elementary level of investigation, *i.e.*, at single jet level? Single quark- and gluon-jets can be isolated as well known in experiments and Monte Carlo simulations using a convenient jet-finding algorithm. The use of these algorithms, although still under discussion, should be considered at present the only way which we have to localize single jet properties from many jet events samples. In this connection, it was interesting to find in Monte Carlo simulations that the

mentioned regularities for clans are valid with a high degree of precision for final hadrons in single jets originated by an initial quark and gluon[8]. The accuracy is again improved by going *via* GLPHD to final parton level.

In parallel, the theoretical study of single parton shower was progressing in the literature[9,10,11,12]. A contribution along this line of thought is the Simplified Parton Shower (SPS) model[13], which describes final parton MD's in a single jet originated by an initial parton assuming that partons are controlled by the dominant interaction among gluons (gluon self-interaction) in a correct kinematical framework. The model was solved numerically and results confirm the relevance of clan structure analysis for discussing final parton MD's properties.

New perspectives on the theoretical basis of clan concept were opened later on by the discovery of its link with void probability in rapidity space, *i.e.*, the probability to detect no particles in a given domain of phase space, and the related hierarchical structure of the corresponding correlation functions[14]: the relevance of clan concept emerged fully within the class of Infinitely Divisible Distributions which reduce to NB MD in a particular case, *i.e.*, the clan concept was found to be more general than NB regularity.

All these undeniable successes notwithstanding, our search failed in explaining the independence of the average number of clans on c.m. energy in a fixed rapidity interval, its linear dependence on rapidity at fixed c.m. energy and its subsequent bending for larger rapidity intervals. To our knowledge, it should be added, these facts are neither explained nor predicted in single parton showers (jets) by any of the existing models in the field.

In order to answer these challenging questions at parton level, we decided to implement clan concept in the SPS model[13]. This generalized version of SPS, which we call Generalized Simplified Parton Shower (GSPS) model goes as follows. We assume that the number of clans in each event coincides with the number of steps of the Markov cascade originated by an initial parton, *i.e.*, at each step in the evolution of a single jet independent intermediate shower sources, the clans, are emitted with degrading virtualities. Consequently, the number of clan ancestors is distributed according to a shifted Poisson distribution. By assuming local fluctuations in virtuality of the initial parton at the origin of the cascade and of clan ancestors, we calculate *analytically* the energy and rapidity dependence of the average number of clans. It is shown that clan properties at partonic single jet level obtained from experimental data and from Monte Carlo simulations via GLPHD are correctly reproduced by our model. A new striking regularity for the

average number of clans is also discovered.

In section **II** we review the structure of the SPS model for single jets; in section **III** we present its generalized version and calculate clan MD's both in full phase space and in symmetric rapidity intervals. Conclusions are drawn at the end.

II. Summary and critical reading of SPS model for single jets.

In this section we examine the main features of SPS model which are relevant for our scope and which we developed in [13]. Our aim was to obtain the virtuality evolution and the rapidity structure of a single parton shower by assuming essentials of QCD and the validity at each step of the cascading process of the energy-momentum conservation law. Inspired by the criterium of maximum simplicity, essential features of QCD which we decided to incorporate in the model are the dominance of gluon self-interaction as described by a kernel of the form suggested in [15] and a Sudakov form factor term in order to normalize the elementary virtuality splitting function. Virtuality evolution in a single jet (parton shower) was then described as follows.

We consider an initial parton of maximum allowed virtuality W which splits at virtuality Q into two partons of virtuality Q_0 and Q_1. We require $Q \geq Q_0 + Q_1$ and $Q_0, Q_1 \geq 1$ GeV. We define the probability for a parton of virtuality W to split at Q, $p(Q|W)$, which is normalized by a Sudakov form factor. The probability for an ancestor parton of maximum allowed virtuality W to generate n final partons, $P_n(W)$, and the probability for a parton which splits at virtuality Q to generate n final partons, $R_n(Q)$, with $R_n(Q) = \delta_{n1}$ for $Q < 2$ GeV, lead to the corresponding generating functions:

$$f(z, W) = \sum_{n=1}^{\infty} P_n(W) z^{n-1} \tag{1}$$

$$g(z, Q) = \sum_{n=2}^{\infty} R_n(Q) z^{n-2} \tag{2}$$

The two generating functions are linked by

$$f(z, W) = \int_1^2 p(Q|W)dQ + \int_2^W p(Q|W)zg(z, Q)dQ \tag{3}$$

The joint probability density $\mathcal{P}(Q_0 Q_1|Q)$ for a parton of virtuality Q to split into two partons of virtuality Q_0 and Q_1 is defined by

$$\mathcal{P}(Q_0 Q_1|Q) = p(Q_0|Q)p(Q_1|Q)K(Q) \tag{4}$$

3

where $K(Q)$ is a normalization factor.

The dynamical content of the model in *virtuality* is contained in the following equation

$$R_n(Q) = \sum_{n'=1}^{n-1} \int_1^\infty dQ_0 \int_1^\infty dQ_1 \mathcal{P}(Q_0 Q_1 | Q) R_{n-n'}(Q_0) R_{n'}(Q_1) \theta(Q - Q_0 - Q_1)$$

(5)

which gives the probability for a parton which splits at virtuality Q to generate n final partons in terms of the joint probability density for a parton of virtuality Q to split into two partons of virtuality Q_0 and Q_1.

Eq. (5) can be reformulated for the corresponding generating function by dividing the domain of integration in three subdomains; one obtains

$$
\begin{aligned}
g(z, Q) = & \int_1^2 dQ_0 \int_1^2 dQ_1 \mathcal{P}(Q_0 Q_1 | Q) \theta(Q - Q_0 - Q_1) + \\
& 2 \int_1^2 dQ_0 \int_2^\infty dQ_1 \mathcal{P}(Q_0 Q_1 | Q) z g(z, Q_1) \theta(Q - Q_0 - Q_1) + \\
& \int_2^\infty dQ_0 \int_2^\infty dQ_1 \mathcal{P}(Q_0 Q_1 | Q) z g(z, Q_0) z g(z, Q_1) \theta(Q - Q_0 - Q_1)
\end{aligned}
$$

(6)

The above three subdomains correspond to the possible different situations in which the two generated partons can be found *i.e.*, no one or only one or both split. This general scheme is valid for any splitting function $p(Q|W)$. In case $p(Q|W)$ is factorizable in terms of its variables Q and W, *i.e.*,

$$p(Q|W) = p_0(Q) C(W), \quad C(W) = \left[\int_1^W dQ' p_0(Q') \right]^{-1}$$

(7)

eq. (3) simplifies into the differential equation

$$\frac{\partial f(z, W)}{\partial W} = p(W|W)[z g(z, W) - f(z, W)]$$

(8)

For numerical simulations we choose:

$$p(Q|W) dQ = \frac{A}{Q} \frac{(\log Q)^{A-1}}{(\log W)^A} dQ = d\left(\frac{\log Q}{\log W} \right)^A$$

(9)

A being the only free parameter of the model. This form of $p(Q|W)$ was motivated in [13] by our request of simplicity in the structure of the model. Notice that eq. (9) corresponds to the virtuality dependence of the standard QCD kernel.

4

For describing the *rapidity* structure of the model, we proposed in [13] to use the singular part of the QCD kernel controlling gluon branching:

$$p(y_0|Q_0Q_1Qy) \propto P(z_0)dz_0 \propto \frac{dz_0}{z_0(1-z_0)} \tag{10}$$

Here z_0 is the energy fraction carried out by the produced parton in the infinite momentum frame.

The limits of variation of z_0 are fixed by the exact kinematical relations

$$B - \sqrt{B^2 - \left(\frac{Q_0}{Q}\right)^2} \leq z_0 \leq B + \sqrt{B^2 - \left(\frac{Q_0}{Q}\right)^2} \tag{11}$$

where $B = \frac{1}{2}[1 + (\frac{Q_0}{Q})^2 - (\frac{Q_1}{Q})^2]$ is the scaled parton energy in the center of mass system and $\sqrt{B^2 - (\frac{Q_0}{Q})^2}$ its maximum scaled transverse momentum. In this way the scaled transverse momentum of the parton with energy fraction z_0

$$\frac{|p_{T0}|^2}{Q^2} = \sqrt{B^2 - \left(\frac{Q_0}{Q}\right)^2} - (z_0 - B)^2 \tag{12}$$

and its rapidity

$$y_0 = y + \frac{1}{2}\log\frac{B + |z_0 - B|}{B - |z_0 - B|} \tag{13}$$

are uniquely determined. Rapidity of the second parton of virtuality Q_1 is obtained by energy-momentum conservation:

$$y_1 = y + \tanh^{-1}\left[\frac{B}{B+1}\tanh|y_0 - y|\right] \tag{14}$$

Notice that only the first step has to be treated differently in rapidity because it corresponds to the degrading from the maximum allowed virtuality W to the virtuality of the first splitting Q. In this case the rapidity of the ancestor is fixed by conservation laws and is given by

$$y = \tanh^{-1}\sqrt{1 - \left(\frac{Q}{W}\right)^2} \tag{15}$$

The kinematical structure of the model is summarized in Figure 1.

The virtuality evolution equations in full phase space have been analytically solved in two cases: a Poissonian distribution has been obtained when only one

5

produced parton can split and a geometric distribution is found when we neglect the virtuality conservation law in the production process.

We found that the numerical solution of the master equation for the MD in a single jet is well reproduced by a NB distribution in full phase space, in symmetric rapidity intervals and in p_T intervals. It is also found that the average number of clans approximately scales with jet energy in a fixed rapidity interval.

At this level of investigation, it should be clear that still open problems are the lack of the analytical solution of equation (6) and, in more general terms, the lack of a complete analytical study of the parton evolution process in rapidity and p_T variables.

III. The Generalized Simplified Parton Shower Model (GSPS)

In order to solve part of the problems indicated at the end of the previous section, we propose to incorporate in the SPS model the clan concept; we call this version of the model Generalized Simplified Parton Shower (GSPS) model. Accordingly, we decide now to pay attention for each event to the ancestor which, splitting n times, gives rise to n subprocesses (one at each splitting) (see Figure 2) and we identify them with clans. Therefore in this model for a single event the concept of clan at parton level is no more as it was in [1], *i.e.*, only a *statistical* one. In the present picture the clans are independent active parton sources and *their number in each event coincides with the number of splittings of the ancestor, i.e., with the number of steps in the cascade.*

Notice that each clan generation is independent of previous history (it has no memory); thus the process is markoffian. Furthermore each generation process depends on the evolution variable only and is independent of the other variables of the process like the number of clans already present and their virtualities. In the original version of SPS the splitting function of the first step, $p(Q_0|Q)$, was different from the splitting function of all the other steps, $\beta(Q_0|Q)$, obtained by integrating the joint probability function $\mathcal{P}(Q_0Q_1|Q)$

$$\beta(Q_0|Q) = \int_1^{Q-Q_0} dQ_1 \mathcal{P}(Q_0Q_1|Q) \tag{16}$$

In order to generalize the SPS model as it stands we assume that virtuality conservation law is locally violated (although conserved globally) according to

$$1 \leq Q_0 \leq Q, \qquad 1 \leq Q_1 \leq Q \tag{17}$$

6

The upper limit of integration of (16) becomes Q, the normalization factor $K(Q)$ reduces to 1 and the process becomes homogeneous in the evolution variable since

$$\beta(Q_0|Q) = p(Q_0|Q) \int_1^Q p(Q_1|Q)dQ_1 = p(Q_0|Q) \tag{18}$$

where $p(Q_0|Q)$ is factorized according to eq. (7). The approximation described by eq. (18), therefore, can be interpreted as the effect of local fluctuations in virtuality occurring at each clan emission.

This violation of the virtuality conservation law spoils of course the validity of the energy-momentum conservation law, which, in the SPS model, uniquely determines the rapidity of a produced parton, given its virtuality and the virtuality and rapidity of its germane parton (see eq. (14)). In the GSPS model the two produced partons at each splitting are independent both in virtuality and in rapidity; however, the rapidity of each parton is bounded by the extension of phase space fixed by its virtuality and the virtuality of the parent parton:

$$|y_i - y| \leq \log \frac{Q}{Q_i} \tag{19}$$

In conclusion, by weakening locally conservation laws, we decouple the production process of partons at each splitting. Consequently, the GSPS model allows to follow just a branch of the splitting, since each splitting can be seen here as the product of two independent parton emissions. This consideration will be particularly useful in discussing the structure in rapidity of the model; in fact, it is implied that the Altarelli-Parisi kernel given in eq. (10) should be identified with

$$p(y_0|Q_0Qy)dy_0 p(y_1|Q_1Qy)dy_1 \propto \frac{dz_0}{z_0} \frac{dz_1}{z_1} \tag{20}$$

In the following we propose to study clan formation in a parton shower first in virtuality variable and, next, in virtuality and rapidity variables. The $p_{_T}$ dependence of clan properties in the GSPS model could be treated with the proper modifications in an analogous way.

In order to stress the fact that from now on we will pay attention to clan production, we use lowercase letters (r,p) when we refer to the probability of producing N clans, whereas in section **II** we used uppercase letters (R,P) for the probability of producing n partons. In addition, in order to be extremely clear, we proceed to calculate first the probability for emitting N clans without including the first step, r_N, and later the same probability by including it, p_N.

III.a. Clans formation in a parton shower: Full Phase Space

Let us consider the probability $r_N(Q_0|Q)$ that an ancestor parton, splitting at virtuality $Q \geq 2$ GeV, gets virtuality Q_0 after emitting $N-1$ clans.

In the GSPS model this probability can be expressed in terms of the elementary splitting function, $p(Q_0|Q)$, (see Figure 3, solid line diagrams):

$$r_0(Q_0|Q) = 0, \qquad r_1(Q_0|Q) = 0, \qquad r_2(Q_0|Q) = p(Q_0|Q),$$

$$r_3(Q_0|Q) = \int_{\max\{2,Q_0\}}^{Q} dQ_1 p(Q_0|Q_1)p(Q_1|Q),$$

$$\vdots \tag{21}$$

$$r_N(Q_0|Q) = \int_{\max\{2,Q_0\}}^{Q} dQ_{N-2} \int_{\max\{2,Q_0\}}^{Q_{N-2}} dQ_{N-3} \dots$$

$$\int_{\max\{2,Q_0\}}^{Q_2} dQ_1 p(Q_0|Q_1)p(Q_1|Q_2)\dots p(Q_{N-2}|Q)$$

Notice that, since a parton of virtuality less than 2 GeV does not split, the probability $r_N(Q_0|Q)$ has a different form when the virtuality Q_0 is larger or smaller than 2 GeV. By taking into account the factorization of $p(Q_0|Q)$ given in eq. (7), eq. (21) can be rewritten as:

$$r_N(Q_0|Q) = p(Q_0|Q) \int_{\max\{2,Q_0\}}^{Q} p(Q_{N-2}|Q_{N-2})dQ_{N-2}$$

$$\int_{\max\{2,Q_0\}}^{Q_{N-2}} p(Q_{N-3}|Q_{N-3})dQ_{N-3} \dots \int_{\max\{2,Q_0\}}^{Q_2} p(Q_1|Q_1)dQ_1 \tag{22}$$

The multiple integral of the product of identical factors over the ordered domain $\max\{2,Q_0\} \leq Q_1 \leq Q_2 \leq \dots \leq Q_{N-2} \leq Q$ can be solved by extending the integration domain to a (N-2)-dimensional hypercube of length $Q - \max\{2,Q_0\}$. Then, by using the symmetry of the integrand, one gets

$$r_N(Q_0|Q) = \begin{cases} p(Q_0|Q)\frac{[\lambda(Q)-\lambda(Q_0)]^{N-2}}{(N-2)!} & Q_0 \geq 2 \text{ GeV} \\ p(Q_0|Q)\frac{[\lambda(Q)]^{N-2}}{(N-2)!} & Q_0 < 2 \text{ GeV} \end{cases} \tag{23}$$

with

$$\lambda(u) \equiv \int_2^u p(u'|u')du'$$

8

The probability $r_N(Q)$ that a parton, splitting at virtuality Q, generates a shower with N clans is given by integrating Q_0 over the range allowed for a final parton:

$$r_N(Q) \equiv \int_1^2 dQ_0 r_N(Q_0|Q) \tag{24}$$

Since only the second of eq. (23) contributes, one obtains a shifted-Poisson distribution

$$r_0(Q) = 0 \qquad r_1(Q) = 0$$
$$r_N(Q) = e^{-\lambda(Q)} \frac{[\lambda(Q)]^{N-2}}{(N-2)!} \qquad N \geq 2 \tag{25}$$

The average number of clans generated by an initial parton splitting at Q follows:

$$\bar{N}_r(Q) \equiv \sum_{N=0}^{\infty} N r_N(Q) = \sum_{N=2}^{\infty} N e^{-\lambda(Q)} \frac{[\lambda(Q)]^{N-2}}{(N-2)!} = \lambda(Q) + 2 \tag{26}$$

Now we can take into account the first step and study the multiplicity distribution for clans produced from an ancestor of maximum allowed virtuality W (see Figure 4, solid line diagrams). The probability that an ancestor parton of maximum virtuality W gets virtuality Q_0 after emitting $N-1$ clans, $p_N(Q_0|W)$, is given by:

$$p_0(Q_0|W) = 0, \qquad p_1(Q_0|W) = p(Q_0|W),$$
$$p_2(Q_0|W) = \int_{\max\{2,Q_0\}}^{W} dQ\, p(Q_0|Q) p(Q|W),$$
$$\vdots \tag{27}$$
$$p_N(Q_0|W) = \int_{\max\{2,Q_0\}}^{W} dQ \int_{\max\{2,Q_0\}}^{Q} dQ_{N-2} \cdots$$
$$\int_{\max\{2,Q_0\}}^{Q_2} dQ_1 p(Q_0|Q_1) p(Q_1|Q_2) \ldots p(Q_{N-2}|Q) p(Q|W)$$

It should be pointed out that eq. (27) for $N \geq 2$ can be obtained also by rewriting $p_N(Q_0|W)$ in terms of $r_N(Q_0|Q)$:

$$p_N(Q_0|W) = \int_{\max\{2,Q_0\}}^{W} dQ\, p(Q|W) r_N(Q_0|Q) \tag{28}$$

This relation for clans corresponds to eq. (3) for partons.

Explicitly,

$$p_N(Q_0|W) = \begin{cases} p(Q_0|W) \frac{[\lambda(W)-\lambda(Q_0)]^{N-1}}{(N-1)!} & Q_0 \geq 2 \text{ GeV} \\ p(Q_0|W) \frac{[\lambda(W)]^{N-1}}{(N-1)!} & Q_0 < 2 \text{ GeV} \end{cases} \tag{29}$$

9

Then, by integrating over Q_0 in the allowed virtuality range, one gets the multiplicity distribution $p_N(W)$:

$$p_0(W) = 0$$

$$p_N(W) \equiv \int_1^2 dQ_0 p_N(Q_0|W) = e^{-\lambda(W)} \frac{[\lambda(W)]^{N-1}}{(N-1)!} \tag{30}$$

Being included in eq. (30) the graph corresponding to the case in which the ancestor does not split (one-parton shower), N starts from 1 and not from 2 as in eq. (26).

Eq. (30) is a shifted Poissonian distribution with average number of clans given by:

$$\bar{N}(W) \equiv \sum_{N=0}^{\infty} N p_N(W) = \sum_{N=1}^{\infty} N e^{-\lambda(W)} \frac{[\lambda(W)]^{N-1}}{(N-1)!} = \lambda(W) + 1 \tag{31}$$

which is fully consistent with eq. (26) via eq. (28). We stress that this result has been obtained *a priori* in the present generalized version of the model, differently from what has been done previously in [1] where the independent production of clans was an "ansatz" introduced *a posteriori* in order to explain the occurrence of NB regularity.

Eqs. (30) and (31) answer to our main questions in full phase space. In order to introduce the subsequent discussion on rapidity dependence, we propose to study first the clan density in virtuality, *i.e.*, the number of clans emitted with virtuality Q_0 from an ancestor parton splitting at virtuality Q.

We start by considering the probability that the $(N-1)^{\text{th}}$ clan is emitted with virtuality Q_0. Now, it should be remarked that in the GSPS model the elementary splitting function for a parent parton of virtuality Q to produce a clan of virtuality Q_1, $p(Q_1|Q)$, has the same functional form of the probability to produce the associated parton of virtuality Q_0, $p(Q_0|Q)$. Therefore, the role played by the ancestor and the clan at the last step of the cascade can be interchanged; the probability that an ancestor, splitting at Q, gets virtuality Q_0 after emitting $N-1$ clans, $r_N(Q_0|Q)$, (see Figure 3, solid line diagrams and eqs. (21,23)) turns out to be equal to the probability to produce the $(N-1)^{\text{th}}$ clan with virtuality Q_0 (see Figure 3, dashed line diagrams). Finally, by summing over N, the average number of clans produced with virtuality Q_0, $r_\Sigma(Q_0|Q)$, is obtained; the explicit expression of this probability is quite subtle, since one has to carefully take into

account the role of the ancestor. For $Q_0 \geq 2$ GeV, the ancestor will generate other partons and will not contribute to the final clan density:

$$r_\Sigma(Q_0|Q) \equiv \sum_{N=2}^{\infty} r_N(Q_0|Q) \qquad Q_0 \geq 2 \text{ GeV} \tag{32}$$

For $Q_0 < 2$ GeV, the ancestor is considered as one parton clan and will contribute to $r_\Sigma(Q_0|Q)$ in addition to the term given in eq. (32); thus one has

$$r_\Sigma(Q_0|Q) \equiv \sum_{N=2}^{\infty} r_N(Q_0|Q) + r_{\text{anc}}(Q_0|Q) \qquad Q_0 < 2 \text{ GeV} \tag{33}$$

where $r_{\text{anc}}(Q_0|Q)$ is the probability to obtain an ancestor of virtuality $Q_0 < 2$ GeV in any number of steps and is given by

$$r_{\text{anc}}(Q_0|Q) = \sum_{N=2}^{\infty} r_N(Q_0|Q) \tag{34}$$

Notice that to eq. (34) will contribute just the second of the two eqs. (23). Accordingly

$$r_{\text{anc}}(Q_0|Q) = \sum_{N=2}^{\infty} p(Q_0|Q) \frac{[\lambda(Q)]^{N-2}}{(N-2)!} = p(Q_0|Q) e^{\lambda(Q)} \tag{35}$$

and the full expression for the clan density in virtuality, $r_\Sigma(Q_0|Q)$, turns out to be

$$r_\Sigma(Q_0|Q) = \begin{cases} p(Q_0|Q) e^{\lambda(Q)-\lambda(Q_0)} & Q_0 \geq 2 \text{ GeV} \\ 2p(Q_0|Q) e^{\lambda(Q)} & Q_0 < 2 \text{ GeV} \end{cases} \tag{36}$$

The consistency of this result can easily be checked: by integrating $r_\Sigma(Q_0|Q)$ over Q_0 in the full domain one should obtain indeed for the average number of clans, $\bar{N}_r(Q)$, the same expression which was calculated in eq. (26). In fact

$$\int_1^Q dQ_0 r_\Sigma(Q_0|Q) = \int_1^2 dQ_0 2p(Q_0|Q) e^{\lambda(Q)} + \int_2^Q dQ_0 p(Q_0|Q) e^{\lambda(Q)-\lambda(Q_0)} =$$
$$= 2 + \lambda(Q) = \bar{N}_r(Q) \tag{37}$$

The same procedure can be used for studying the density of clan produced by an ancestor of maximum allowed virtuality W. We start by considering the probability to produce the $(N-1)^{\text{th}}$ clan at virtuality Q_0 from the ancestor of maximum allowed virtuality W (see Figure 4, dashed line diagrams). In the model this probability turns out to be equal to the probability that the ancestor of maximum

11

allowed virtuality W gets virtuality Q_0 after emitting $N - 1$ clans, *i.e.*, to the probability $p_N(Q_0|W)$ given by eq. (29) (in Figure 4, solid line diagrams).

Notice that the showers with one parton only do not spoil our reasoning; however, they will contribute to the average number of clans produced with virtuality Q_0, $p_\Sigma(Q_0|W)$, for $Q_0 < 2$ GeV. It follows

$$p_\Sigma(Q_0|W) = \begin{cases} \sum_{N=2}^{\infty} p_N(Q_0|W) & Q_0 \geq 2 \text{ GeV} \\ \sum_{N=2}^{\infty} p_N(Q_0|W) + p_{\text{anc}}(Q_0|W) & Q_0 < 2 \text{ GeV} \end{cases} \quad (38)$$

where $p_{\text{anc}}(Q_0|W)$ is given by definition by

$$p_{\text{anc}}(Q_0|W) = \sum_{N=1}^{\infty} p_N(Q_0|W) = \sum_{N=1}^{\infty} p(Q_0|W)\frac{[\lambda(W)]^{N-1}}{(N-1)!}$$
$$= p(Q_0|W)e^{\lambda(W)} \quad (39)$$

The sum starts of course from $N = 1$ since, as we discussed previously, we must include the contribution of one-parton showers.

Accordingly, one has:

$$p_\Sigma(Q_0|W) = \begin{cases} p(Q_0|W)\left[e^{\lambda(W)-\lambda(Q_0)} - 1\right] & Q_0 \geq 2 \text{ GeV} \\ p(Q_0|W)\left[2e^{\lambda(W)} - 1\right] & Q_0 < 2 \text{ GeV} \end{cases} \quad (40)$$

The consistency of our calculation can be checked by integrating eq. (40) over Q_0 from 1 to W; eq. (31) follows.

Eq. (31) solves our first problem to determine analytically the average number of clans generated by an initial parton of maximum allowed virtuality W in full phase space. It should be added that eq. (36) and eq. (40) are simply connected by the relation

$$p_\Sigma(Q_0|W) = \begin{cases} \int_{Q_0}^{W} dQ\, p(Q|W) r_\Sigma(Q_0|Q) & Q_0 \geq 2 \text{ GeV} \\ \int_{2}^{W} dQ\, p(Q|W) r_\Sigma(Q_0|Q) + p(Q_0|W) & Q_0 < 2 \text{ GeV} \end{cases} \quad (41)$$

which is obtained by introducing eqs. (28), (32) and (39) into eq. (38).

In the following subsection, eq. (41) will be extended to include rapidity variable in order to calculate the average number of clans in symmetric rapidity intervals.

III.b. Clans formation in a parton shower: Symmetric rapidity intervals

In this subsection we extend our study to clan distributions in symmetric rapidity intervals $\Delta y = [-y_c, y_c]$. We relate the probability to have N' clans in

the symmetric rapidity interval Δy, $p_{N'}(y_c, W)$, to the corresponding probability defined in full phase space (fps), $p_N(W)$, by using the following relation

$$p_{N'}(y_c, W) = \sum_{N=N'}^{\infty} \Pi(N', y_c|N, \text{fps})p_N(W) \tag{42}$$

where $\Pi(N', y_c|N, \text{fps})$ is the conditional probability to have N' clans in Δy when one has N clans in full phase space; it contains all dynamical information on the *rapidity structure* of the production process.

Following the discussion in subsection *III.a* and in particular the fact that *clans are not correlated in full phase space and the only allowed correlations are among particles within the same clan*, the conditional probability $\Pi(N', y_c|N, \text{fps})$ turns out to be a positive binomial distribution

$$\Pi(N', y_c|N, \text{fps}) = \binom{N}{N'} \pi^{N'}(1 - \pi)^{N-N'} \tag{43}$$

where $\pi(y_c, W)$ is the probability to produce a single clan in the rapidity interval Δy from the maximum allowed virtuality W. In terms of generating functions $f_{\text{clan}}(z) \equiv \sum_{N=0}^{\infty} p_N z^N$, the above relation can be written as

$$f_{\text{clan}}^{\Delta y}(z) = f_{\text{clan}}^{\text{fps}}(\pi z + 1 - \pi) \tag{44}$$

Being clans distributed in full phase space according to a shifted Poisson distribution (eq. (30)), *via* eq. (44), the probability generating function for clans in symmetric rapidity intervals has the following form

$$f_{\text{clan}}^{\Delta y}(z) = \left[\pi(y_c, W)z + 1 - \pi(y_c, W)\right] e^{\lambda(y_c, W)(z-1)} \tag{45}$$

where $\lambda(y_c, W) = \pi(y_c, W)\lambda(W)$.

Eq. (45), being the sum of two Poissonian distribution (the first a shifted one), has a nice physical meaning: the two terms correspond to the probability of having the ancestor within or outside the given rapidity interval. Since in full phase space $\pi(y_c = \text{fps}, W) = 1$, from eq. (45) one obtains the generating function for full phase space. In addition, it should be pointed out that the void probability in a given rapidity interval, $p_0(y_c, W)$, is different from zero and is given by

$$p_0(y_c, W) = \left[1 - \pi(y_c, W)\right] e^{-\pi(y_c, W)\lambda(W)} \tag{46}$$

When y_c is very small, $\pi(y_c, W)$ tends to zero and the unshifted Poissonian dominates. Thus, it can be stated that in the smallest rapidity intervals the clan

multiplicity is to a good approximation Poissonian and the full MD belongs to the class of Compound Poisson Distribution[14]. $\pi(y_c, W)$ tends to 1 for y_c at the border of phase space and the exact full phase space shifted-Poisson distribution is approached. Finally, when $\lambda(y_c, W)$ is sufficiently large, the shifted-Poissonian dominates at large N (the tail of the distribution) while the unshifted one dominates at small N (the head of the distribution). These facts might have some consequences in interpreting the anomalies found in NB behavior for small N and the deviations from NB behavior in large rapidity intervals, which are controlled by the behavior of the distribution at large N.

From eq. (45) it follows that the average number of clans is given by:

$$\bar{N}(y_c, W) = \pi(y_c, W)\bar{N}(W) \tag{47}$$

We are ready now to calculate the average number of clans in symmetric rapidity intervals.

The probability that the ancestor, splitting at virtuality Q and rapidity y, gets virtuality Q_0 and rapidity y_0 emitting $N-1$ clans, $r_N(Q_0 y_0 | Q y)$, can be expressed within the GSPS model (as for $r_N(Q_0|Q)$) in terms of elementary splitting functions according to the following formula (see Figure 3, solid line diagrams):

$$r_N(Q_0 y_0 | Q y) = \int_{\max\{2, Q_0\}}^{Q} dQ_{N-2} \ldots \int_{\max\{2, Q_0\}}^{Q_2} dQ_1 p(Q_0|Q_1) \ldots p(Q_{N-2}|Q)$$
$$\int_{-\infty}^{\infty} dy_{N-2} \ldots \int_{-\infty}^{\infty} dy_1 Y(|y_0 - y_1|, Q_0, Q_1) \ldots Y(|y_{N-2} - y|, Q_{N-2}, Q)$$
$$\tag{48}$$

where $Y(|y_i - y_{i+1}|, Q_i, Q_{i+1})$ is the probability that a parent parton with rapidity y_{i+1} generates in a single step a parton of rapidity y_i, being their virtualities Q_{i+1} and Q_i respectively.

Inspired by the criterium of simplicity which we decided to follow from the beginning of our work and by the considerations discussed at the beginning of Section **III**, we take for the probability $Y(|y_i - y_{i+1}|, Q_i, Q_{i+1})$ the simplified QCD-splitting kernel

$$Y(|y_i - y_{i+1}|, Q_i, Q_{i+1}) dy_i = P(z_i) dz_i \propto \frac{dz_i}{z_i} \tag{49}$$

By using eq. (13) properly rewritten, the kernel becomes

$$Y(|y_i - y_{i+1}|, Q_i, Q_{i+1}) dy_i \propto dy_i \tag{50}$$

which after the normalization in the kinematically allowed domain $|y_i - y_{i+1}| \leq \log(Q_{i+1}/Q_i)$ turns out to be:

$$Y(|y_i - y_{i+1}|, Q_i, Q_{i+1})dy_i = \frac{dy_i}{2\log\left(\frac{Q_{i+1}}{Q_i}\right)}\theta(\log(Q_{i+1}/Q_i) - |y_i - y_{i+1}|) \quad (51)$$

Notice that in the limit of $Q_{i+1} \to Q_i$ the function $Y(|y_i - y_{i+1}|, Q_i, Q_{i+1})$ reduces to a Dirac δ-function; moreover, by inserting eq. (51) into eq. (48) and by integrating over y_0 in all the allowed domain one recovers immediately the full phase space result given in eq. (21).

In this equation, as well as in the case of full phase space, one can identify the probability $r_N(Q_0 y_0 | Qy)$ with the probability that the $(N-1)^{\text{th}}$ clan is produced with virtuality Q_0 and rapidity y_0 from an ancestor which splits at virtuality Q and rapidity y (see Figure 3, dashed line diagrams).

The integrations in the allowed domain in rapidity of eq. (48) are awkward and quite difficult. The idea is to approximate the probability density given by eq. (51) with a gaussian of the following form:

$$Y(|y_i - y_{i+1}|, Q_i, Q_{i+1}) = \frac{1}{\sqrt{2\pi}\sigma_i}\exp\left(-\frac{|y_i - y_{i+1}|^2}{2\sigma_i^2}\right) \quad (52)$$

σ_i^2 being the width of the distribution given by

$$\sigma_i^2 \propto \log\left(\frac{Q_{i+1}}{Q_i}\right) = \alpha\log\left(\frac{Q_{i+1}}{Q_i}\right) \quad (53)$$

This approximation corresponds to weaken locally energy-momentum conservation laws and simulates the onset of local fluctuations on the probability density defined by eq. (51). It is remarkable that with the just mentioned simplification the integrations on the rapidity domains can easily be performed and lead to the following result:

$$\int_{-\infty}^{\infty} dy_{N-2}\ldots\int_{-\infty}^{\infty} dy_1 Y(|y_0 - y_1|, Q_0, Q_1)\ldots Y(|y_{N-2} - y|, Q_{N-2}, Q) =$$

$$= \frac{1}{\sqrt{2\pi}\left(\sum_{i=0}^{N-2}\sigma_i^2\right)^{1/2}}\exp\left(-\frac{|y_i - y_{i+1}|^2}{2\sum_{i=0}^{N-2}\sigma_i^2}\right) \quad (54)$$

From eq. (53), one sees that the width of the right part of eq. (54) depends only on initial and final virtualities, $i.e.$,

$$\sum_{i=0}^{N-2}\sigma_i^2 = \alpha\sum_{i=0}^{N-2}(\log Q_{i+1} - \log Q_i) = \alpha\log\left(\frac{Q}{Q_0}\right) \quad (55)$$

15

It is clear that eq. (48) can be written now in terms of the probability $r_N(Q_0|Q)$ defined in eq. (21) as follows:

$$
\begin{aligned}
r_N(Q_0y_0|Qy) &= Y(|y_0 - y|, Q_0Q) \int_{\max\{2,Q_0\}}^{Q} dQ_{N-2} \ldots \\
&\qquad \int_{\max\{2,Q_0\}}^{Q_2} dQ_1 p(Q_0|Q_1) \ldots p(Q_{N-2}|Q) \\
&= Y(|y_0 - y|, Q_0Q) \times r_N(Q_0|Q)
\end{aligned}
\tag{56}
$$

By recalling eq. (23), one has:

$$
r_N(Q_0y_0|Qy) = \begin{cases} p(Q_0|Q)Y(|y_0 - y|, Q_0Q)\frac{[\lambda(Q) - \lambda(Q_0)]^{N-2}}{(N-2)!} & Q_0 \geq 2 \;\; \text{GeV} \\ p(Q_0|Q)Y(|y_0 - y|, Q_0Q)\frac{[\lambda(Q)]^{N-2}}{(N-2)!} & Q_0 < 2 \;\; \text{GeV} \end{cases}
\tag{57}
$$

In summary, the use of gaussian approximation for the step function (step function → gaussian) allows to see that the convolution of a generic number of distributions in rapidity domains given by the corresponding step functions is equivalent to a single gaussian distribution in rapidity. If we assume that this approximation can work the other way around (gaussian → step function) the initial form of the probability density $Y(|y_i - y_{i+1}|, Q_i, Q_{i+1})$ as given by eq. (51) is re-obtained restoring the correct kinematical domain for the total distribution.

From eq. (57), it is quite easy to calculate the clan density in virtuality and rapidity produced by an ancestor which splits at virtuality Q and rapidity y. Once again, in this case the ancestor plays a very peculiar role: for $Q_0 \geq 2$ GeV (the ancestor does not contribute) one has

$$
r_\Sigma(Q_0y_0|Qy) \equiv \sum_{N=2}^{\infty} r_N(Q_0y_0|Qy) \qquad Q_0 \geq 2 \text{ GeV}
\tag{58}
$$

and for $Q_0 < 2$ GeV (the ancestor contributes additively) the probability becomes

$$
r_\Sigma(Q_0y_0|Qy) \equiv \sum_{N=2}^{\infty} r_N(Q_0y_0|Qy) + r_{\text{anc}}(Q_0y_0|Qy)
\tag{59}
$$

where $r_{\text{anc}}(Q_0y_0|Qy)$ is given by definition by

$$
r_{\text{anc}}(Q_0y_0|Qy) = \sum_{N=2}^{\infty} r_N(Q_0y_0|Qy)
\tag{60}
$$

16

i.e.,

$$r_\Sigma(Q_0 y_0 | Q y) = 2 \sum_{N=2}^{\infty} r_N(Q_0 y_0 | Q y) \qquad\qquad Q_0 < 2 \text{ GeV} \qquad\qquad (61)$$

Finally, we find

$$r_\Sigma(Q_0 y_0 | Q y) = \begin{cases} p(Q_0|Q) Y(|y_0 - y|, Q_0 Q) e^{\lambda(Q) - \lambda(Q_0)} & Q_0 \geq 2 \text{ GeV} \\ 2 p(Q_0|Q) Y(|y_0 - y|, Q_0 Q) e^{\lambda(Q)} & Q_0 < 2 \text{ GeV} \end{cases} \qquad (62)$$

Clan density in rapidity is calculated by integrating the above density over the virtuality Q_0 in the full virtuality range:

$$r_\Sigma(y_0 | Q y) \equiv \int_1^Q dQ_0 \, r_\Sigma(Q_0 y_0 | Q y) \qquad\qquad (63)$$

Let us study separately this integral for $Q_0 < 2$ GeV and $Q_0 \geq 2$ GeV, *i.e.*,

$$r_\Sigma(y_0 | Q y) \equiv r_{\Sigma, Q_0 < 2} + r_{\Sigma, Q_0 \geq 2} \qquad\qquad (64)$$

For $Q_0 < 2$ GeV one has

$$r_{\Sigma, Q_0 < 2} = 2 \int_1^2 dQ_0 \, p(Q_0|Q) Y(|y_0 - y|, Q_0 Q) e^{\lambda(Q)} =$$

$$= 2 e^{\lambda(Q)} \int_1^2 \frac{dQ_0}{Q_0} \frac{A (\log Q_0)^{A-1}}{(\log Q)^A} \frac{1}{2 \log\left(\frac{Q}{Q_0}\right)} \theta\left(\log\left(\frac{Q}{Q_0}\right) - |y_0 - y|\right) \qquad (65)$$

By defining then $\log Q_0 / \log Q \equiv x$, equation (65) can be rewritten as

$$r_{\Sigma, Q_0 < 2} = A \frac{(\log Q)^{A-1}}{(\log 2)^A} \int_0^{\min(\log 2 / \log Q, 1 - |y_0 - y| / \log Q)} dx \frac{x^{A-1}}{1 - x} \qquad (66)$$

Notice that the integral in eq. (66) can be expressed as a series, *i.e.*:

$$\int dx \frac{x^{A-1}}{1 - x} = \sum_{n=0}^{\infty} \frac{x^{A+n}}{A + n} \qquad\qquad (67)$$

As an example, let us consider the solution of eq. (66) corresponding to $A=2$. One gets:

$$r_{\Sigma, Q_0 < 2} = \frac{2 \log Q}{[\log 2]^2} \left[-\frac{\log 2}{\log Q} - \log\left(1 - \frac{\log 2}{\log Q}\right) \right]$$

$$\text{for } |y_0 - y| \leq \log Q - \log 2$$

$$r_{\Sigma, Q_0 < 2} = \frac{2 \log Q}{[\log 2]^2} \left[-1 + \frac{|y_0 - y|}{\log Q} - \log\left(\frac{|y_0 - y|}{\log Q}\right) \right]$$

$$\text{for } |y_0 - y| > \log Q - \log 2$$

$$(68)$$

Coming now to the second term of eq. (64) ($Q_0 \geq 2$ GeV), one has

$$r_{\Sigma, Q_0 \geq 2} = \int_2^Q dQ_0 p(Q_0|Q) Y(|y_0 - y|, Q_0 Q) e^{\lambda(Q) - \lambda(Q_0)} =$$

$$= \int_2^Q \frac{dQ_0}{Q_0} \frac{A(\log Q_0)^{A-1}}{(\log Q)^A} e^{\lambda(Q) - \lambda(Q_0)} \frac{1}{2 \log \left(\frac{Q}{Q_0} \right)} \theta \left(\log \left(\frac{Q}{Q_0} \right) - |y_0 - y| \right) =$$

$$= \int_2^Q \frac{A dQ_0}{Q_0 \log Q_0} \frac{1}{2 \log \left(\frac{Q}{Q_0} \right)} \theta \left(\log \left(\frac{Q}{Q_0} \right) - |y_0 - y| \right)$$

(69)

In terms of x, this equation can be rewritten as

$$r_{\Sigma, Q_0 \geq 2} = \frac{A}{2 \log Q} \int_{\log 2 / \log Q}^{1 - |y_0 - y| / \log Q} dx \frac{1}{x(1-x)}$$

(70)

Notice that the integral diverges for $x \to 1$, *i.e.*, for $|y_0 - y| = 0$. However, this singularity is under control: it is originated by our choice to follow just one branch of the splitting process, thus allowing $Q_0 \to Q$. Although the probability density is infinite for $|y_0 - y| = 0$, the resulting probability is finite for any finite range of y_0. Therefore, one has

$$r_{\Sigma, Q_0 \geq 2} = \frac{A}{2 \log Q} \log \left[\left(\frac{\log Q - |y_0 - y|}{|y_0 - y|} \right) \left(\frac{\log Q - \log 2}{\log 2} \right) \right], \qquad |y_0 - y| > 0$$

(71)

The expression of Eq. (71) corresponding to $A = 2$ is trivial.

It should be noticed that Eq. (71) is defined in the kinematically allowed region

$$0 < |y_0 - y| \leq \log Q - \log 2 ,$$

(72)

to be compared with the kinematically aloowed region of Eq. (65) ($|y_0 - y| \leq \log Q$).

In conclusion, by adding eqs. (65) and (71) one obtains $r_\Sigma(y_0|Qy)$, the number of clans of rapidity y_0 generated from an ancestor splitting at virtuality Q and rapidity y. The density of clans generated from an ancestor of maximum allowed virtuality W, $p_\Sigma(y_0|W)$, can be studied by integrating over Q in the region shown in Figure 5 (see eq. (41) where analogous calculations are performed in full phase space). The solid line inside the (y_0, Q)-domain in Figure 5 corresponds to eq. (15). It follows

$$p_\Sigma(y_0|W) = \int_2^W dQ p(Q|W) r_\Sigma(y_0|Qy) + p_{\text{anc}}(y_0|W)$$

(73)

18

$p_{\mathrm{anc}}(y_0|W)$ being the probability that the ancestor does not split and has rapidity y_0 fixed by eq. (15):

$$p_{\mathrm{anc}}(y_0|W) = \int_1^2 dQ_0 p(Q_0|W)\delta\left(y_0 - \tanh^{-1}\sqrt{1-(Q_0/W)^2}\right) \qquad (74)$$

This contribution corresponds to the first diagram of Figure 4 and to the thick solid line in the lowest right corner of the (y_0, Q) domain of Figure 5. The δ-function in eq. (74) can be rewritten in terms of Q_0

$$\delta\left(y_0 - \tanh^{-1}\sqrt{1-(Q_0/W)^2}\right) = \delta\left(Q_0 - \frac{W}{\cosh y_0}\right)\frac{W\sinh y_0}{\cosh^2 y_0} \qquad (75)$$

and eq. (74) becomes

$$p_{\mathrm{anc}}(y_0|W) = A\tanh y_0 \frac{[\log W - \log\cosh y_0]^{A-1}}{(\log W)^A}$$
$$\text{for } \tanh^{-1}\sqrt{1-(2/W)^2} \le y_0 \le \tanh^{-1}\sqrt{1-(1/W)^2} \qquad (76)$$

The density of clans in rapidity produced from an ancestor of maximum allowed virtuality W can now be calculated by using Eq. (73). Accordingly, the average number of clans in symmetric rapidity intervals is given by:

$$\bar{N}(y_c, W) \equiv \int_{-y_c}^{y_c} dy_0 p_\Sigma(y_0|W) \qquad (77)$$

This result is remarkable. It should be pointed out that it depends on parameter A only. Parameter A controls – as we have seen in [13] – the number of clans produced in full phase space, *i.e.*, the length of the cascade (since the number of clans in GSPS model is identified with the number of steps in the shower, more steps we have more extended turns out to be the shower). Analytical solutions of eq. (77) can be obtained explicitly for all integer positive values of parameter A, and numerical solutions can be computed for all positive real values of A. We decided to postpone the discussion on the A-dependence of our formula to a forthcoming paper and to limit ourselves to indicate the structure of our formulae by solving analytically the case $A = 2$. This limitation does not alter the main features of our results; in fact preliminary analysis shows that our results are qualitatively not altered by other choices of parameter A. In order to perform the integration, we used the approximation

$$\tanh^{-1}\sqrt{1-\left(\frac{Q}{W}\right)^2} \simeq \log W + \log 2 - \log Q \qquad (78)$$

19

which slightly modifies the (y_0, Q) domain (solid line in Figure 5) into the dashed lines in the same Figure. We summarize in the Appendix the long and cumbersome calculations which are needed in order to integrate eq. (77).

In Figure 6 the clan density $p_\Sigma(y_0|W)$ corresponding to eq. (73) is shown as a function of y_0 variable for maximum allowed virtualities $W = 50$ GeV, $W = 100$ GeV and $W = 500$ GeV. The contribution of one-parton showers turns out to be negligible for this choice of the A value. Notice that the height of the curve is decreasing and the width increasing with the energy. Convolution of clan density for two parton showers is shown in Figure 7. Notice that the central dip at $y \simeq 0$ is slowly removed by increasing the energy of the initial parton. It should be kept in mind that the structure of Figures 6 and 7 refers to clan production; found different behavior for parton production is not in contradiction with this behavior since we have still to include in our scheme parton production within a single clan.

In Figure 8 the average number of clans $\bar{N}(y_c, W)$ (eq. (77)) is given as a function of rapidity width y_c for the same W values of Figure 6. Limitations on the rapidity intervals are determined by the available phase space corresponding to the different initial parton virtualities.

Accordingly, the GSPS model predicts for the average number of clans $\bar{N}(y_c, W)$ at parton level in a single shower (jet):

a) a rising in rapidity width y_c for different initial parton virtualities W very close to linear for $1 < y_c < y_{\text{fps}}$; the rising is still linear but with a somewhat different slope for $y_c < 1$. Characteristic bending occurs finally for rapidity width $y_c \lesssim y_{\text{fps}}$;

b) approximate (into 5%) energy independence in a fixed rapidity interval y_c for W below 100 GeV. For higher virtualities deviations from energy independence become larger; they are into 20% when comparing $\bar{N}(y_c, 50 \text{ GeV})$ and $\bar{N}(y_c, 500 \text{ GeV})$. It should be noticed that the average number of clans slowly decreases with virtuality; this behavior has been already observed in Monte Carlo simulations for single gluon jets[8,16].

In addition to the above results which are consistent with our expectations on clan properties in parton showers, the model shows energy independent behavior (see Figure 9) by normalizing the average number of clans produced in a fixed rapidity interval $|y| \leq y_c$ to the corresponding average number in full phase space, and by expressing this ratio as a function of the rescaled rapidity variable $y_c^* \equiv$

20

y_c/y_{fps}:

$$\pi^*(y_c^*, W) \equiv \frac{\bar{N}(y_c^* \, y_{\text{fps}}, W)}{\bar{N}(W)} \tag{79}$$

This new regularity turns out to be stable for different choices of the parameter A. In Figure 9 a clean linear behavior is shown for the above ratio corresponding to the parameter value $A=2$.

It should be pointed out that the asymptotic ($\log W \to \infty$) expression of the average number of clans for $A = 2$ corresponding to the interval $\log 2 < y_c < \log W - 2\log 2$, which covers almost all the available phase space, is given by

$$
\begin{aligned}
\bar{N}(y_c, W) \simeq \, &2y_c \frac{2\log 2 + \log(\log W/\log 2)}{\log W} + \\
&+ \frac{2}{(\log W)^2}\left[-\frac{11}{3}y_c \log 2 + \frac{4}{3}y_c(\log 2)^2 - 3y_c \log 2 \log(\log W) + \right. \\
&\left. + \, y_c \log 2 \log(\log 2) - \frac{1}{2}\left(y_c - \log 2\right)^2 \log(y_c - \log 2) + \right. \\
&\left. + \frac{1}{2}\left(y_c + \log 2\right)^2 \log(y_c + \log 2) \right] + \mathcal{O}\left(\frac{1}{\log W}\right)^3
\end{aligned} \tag{80}
$$

Eq. (80) can be obtained from eq. (A8) in the Appendix. To first order this formula shows that asymptotically the average number of clans in a fixed rapidity interval grows linearly with y_c and is slowly decreasing with the energy of the initial parton. By including second order contribution, $\bar{N}(y_c, W)$ continues to be linear in y_c and to decrease with the energy but the slope of the curve is different from that at first order; this difference is quite remarkable (a factor 1.5) at low energies (below 100 GeV), but decreases at high energies. Notice that eq. (80) describes perfectly well the result for the average number of clans obtained by using the complete formula discussed in the Appendix in the same rapidity domain.

The asymptotic expression ($\log W \to \infty$) of $\pi^*(y_c^*, W)$ is given by

$$
\begin{aligned}
\pi^*(y_c^*, W) \simeq \, &\frac{2y_c^* \log\left(\frac{\log W}{\log 2}\right)}{1 + 2\log\left(\frac{\log W}{\log 2}\right)} \\
&+ \frac{[(y_c^*)^2 - 1]\log(1 - y_c^*) - (1 + y_c^*)^2 \log(1 + y_c^*)}{1 + 2\log\left(\frac{\log W}{\log 2}\right)} + \\
&+ \frac{4y_c^* \log 2 + (y_c^*)^2}{1 + 2\log\left(\frac{\log W}{\log 2}\right)} + \mathcal{O}(\frac{1}{\log W \log \log W})
\end{aligned} \tag{81}
$$

Eq. (81) describes into 2% the result obtained by using the complete formula after inserting eq. (A8) into eq. (79). It should be pointed out that this behavior is maintained even at higher energies, indicating a scaling behavior in a wide energy range ($50 \div 500000$ GeV). In the limit $W \to \infty$, eq. (81) becomes

$$\pi^*(y_c^*, W) \simeq y_c^* + \mathcal{O}(\frac{1}{\log \log W}) \tag{82}$$

It should be noticed that the slope of this curve is 10% less than that predicted by eq. (81), showing that the asymptotic regime is reached very late.

Conclusions

We have discussed a simplified model, based on essentials of QCD and local weakening of conservation laws for a shower (jet) originated by a parton of given maximum allowed virtuality and given rapidity. It generalizes previous results to the case in which rapidity is added to virtuality evolution by assuming that clans are intermediate independent parton sources; clan production in this framework can be described as a Markoffian process. The new model, which we called Generalized Simplified Parton Shower model (GSPS), allows to determine clan multiplicity distribution in full phase space, which turns out to be a shifted Poissonian to be compared with the Poissonian behavior assumed in the standard interpretation of NB regularity. For clan multiplicity distributions in symmetric rapidity intervals, we obtain a combination of two Poissonian distributions. It is remarkable that the model predicts clan properties which show the same qualitative general trend observed both in experimental data and in Monte Carlo simulations. In addition it has been shown that the ratio $\bar{N}(y_c^* \ y_{\text{fps}}, W)/\bar{N}(W)$ is linear and energy independent when plotted as a function of rescaled rapidity variable y_c^*.

In this paper attention has been payed to the average number of clans produced in a given rapidity interval by an initial parton of maximum allowed virtuality W, $\bar{N}(y_c, W)$; the next step in our program is to calculate the corresponding average number of partons per clan in the same rapidity intervals, $\bar{n}_c(y_c, W)$. We decided to postpone this calculation in the framework of the GSPS to a forthcoming paper.

Appendix

In this Appendix we present a short discussion of the calculation of the integrals given in eqs. (73) and (77) for $A = 2$. Although the integration of the

densities $r_\Sigma(y_0|Qy)$ and $p_\Sigma(y_0|W)$ might be considered straightforward, it is indeed complicated by the appearance of very many terms. They correspond in case of $r_\Sigma(y_0|Qy)$ (eqs. (68) and (71)) to four regions of phase space which, according to Figure 10, we label with Roman letters. They are

$$
\begin{aligned}
&[a] & y - \log Q < y_0 < y - \log Q + \log 2 \\
&[b] & y - \log Q + \log 2 < y_0 < y \\
&[c] & y < y_0 < y + \log Q - \log 2 \\
&[d] & y + \log Q - \log 2 < y_0 < y + \log Q
\end{aligned} \tag{A1}
$$

The densities $r_\Sigma(y_0|Qy)$ are different in the regions [a],[b], [c],[d], and given by:

$$
\begin{aligned}
r_\Sigma[a] = {} & \frac{2}{(\log W)^2} \frac{2}{(\log 2)^2} \Bigg[(\log 2W - y_0)\log Q + (\log Q)^2 \log\log Q + \\
& - 2(\log Q)^2 - (\log Q)^2 \log(\log 2W - y_0 - \log Q) \Bigg]
\end{aligned} \tag{A2}
$$

$$
\begin{aligned}
r_\Sigma[b] = {} & \frac{2}{(\log W)^2} \Bigg[-\frac{2\log Q}{\log 2} - \frac{2(\log Q)^2 \log(\log Q - \log 2)}{(\log 2)^2} + \\
& + \frac{2(\log Q)^2 \log\log Q}{(\log 2)^2} + \log(2\log Q + y_0 - \log 2W) + \\
& - \log(\log 2W - y_0 - \log Q) + \log(\log Q - \log 2) - \log\log 2 \Bigg]
\end{aligned} \tag{A3}
$$

$$
\begin{aligned}
r_\Sigma[c] = {} & \frac{2}{(\log W)^2} \Bigg[-\frac{2\log Q}{\log 2} - \frac{2(\log Q)^2 \log(\log Q - \log 2)}{(\log 2)^2} + \\
& + \frac{2(\log Q)^2 \log\log Q}{(\log 2)^2} + \log(\log 2W - y_0) + \\
& - \log(y_0 - \log 2W + \log Q) + \log(\log Q - \log 2) - \log\log 2 \Bigg]
\end{aligned} \tag{A4}
$$

$$
\begin{aligned}
r_\Sigma[d] = {} & \frac{2}{(\log W)^2} \frac{2}{(\log 2)^2} \Bigg[(y_0 - \log 2W)\log Q + \\
& - (\log Q)^2 \log(y_0 - \log 2W + \log Q) + (\log Q)^2 \log\log Q \Bigg]
\end{aligned} \tag{A5}
$$

where the approximation defined in eq. (78) for y has been used.

Accordingly, the density $p_\Sigma(y_0|W)$ of eq. (73) results to be different in the above mentioned regions. Its integration over y_0 variable leads to divide the integration domain into five regions which we label by Greek letters in Figure 10,

i.e.:

$$(\alpha) \qquad -\log W + \log 2 < y_0 < -\log W + 2\log 2$$

$$(\beta) \qquad -\log W + 2\log 2 < y_0 < \log 2$$

$$(\gamma) \qquad \log 2 < y_0 < \log W - \log 2 \qquad (A6)$$

$$(\delta) \qquad \log W - \log 2 < y_0 < \log W$$

$$(\epsilon) \qquad \log W < y_0 < \log W + \log 2$$

The analytic solution of the integral in eq. (77) turns out to be different for y_c in the following different domains:

$$y_c < \log 2$$
$$\log 2 < y_c < \log W - 2\log 2$$
$$\log W - 2\log 2 < y_c < \log W - \log 2 \qquad (A7)$$
$$\log W - \log 2 < y_c < \log W$$
$$\log W < y_c < \log W + \log 2$$

In order to give the flavor of the cumbersome and long calculations which lead to the final form of $\bar{N}(y_c, W)$, whose asymptotic expression has been given in eq. (80), we show the result for y_c in the domain $\log 2 < y_c < \log W - 2\log 2$, *i.e.*:

$$\bar{N}(y_c, W) = \frac{2}{(\log W)^2} \left\{ \frac{\log W \, \log 2}{2} + \frac{(\log 2)^2}{2} + \frac{5 \, y_c, \log W}{3} - \frac{y_c \, (\log W)^2}{3 \, \log 2} + \right.$$

$$\frac{7 \, y_c \, \log 2}{6} + 2 \, y_c \, \log W \, \log 2 + \frac{4 \, y_c \, (\log 2)^2}{3} + \frac{y_c^2}{2} + \frac{y_c^3}{3 \, \log 2} +$$

$$\left((\log W)^2 + \frac{4 \, y_c \, (\log W)^3}{3 \, (\log 2)^2} \right) \log(\log W) +$$

$$\left(2 \, y_c \, \log W - \frac{4 \, y_c \, (\log W)^3}{3 \, (\log 2)^2} - \frac{2 \, y_c \, \log 2}{3} \right) \log(\log W - \log 2) +$$

$$(-\log W + \log 2) \, y_c \, \log(\log 2) +$$

$$\frac{(-\log W + y_c)^2}{6 \, (\log 2)^2} \left(-(\log W)^2 - 4 \, \log W \, \log 2 - 3 \, (\log 2)^2 + 2 \, y_c \, \log W + \right.$$

$$\left. 4 \, y_c \, \log 2 - y_c^2 \right) \log(\log W - y_c) -$$

$$\frac{(-\log W + \log 2 + y_c)^2 \, \log(\log W - \log 2 - y_c)}{4} +$$

$$\frac{\log(\log W + \log 2 - y_c)}{12 \, (\log 2)^2} \left[2 \, (\log W)^4 + 8 \, (\log W)^3 \, \log 2 + 3 \, (\log W)^2 \, (\log 2)^2 + \right.$$

$$2 \, \log W \, (\log 2)^3 + 5 \, (\log 2)^4 - 8 \, y_c \, (\log W)^3 - 24 \, y_c \, (\log W)^2 \, \log 2 -$$

$$18 \, y_c \, \log W \, (\log 2)^2 - 14 \, y_c \, (\log 2)^3 + 12 \, (\log W)^2 \, y_c^2 + 24 \, y_c^2 \, \log W \, \log 2 +$$

$$\left. 15 \, y_c^2 \, (\log 2)^2 - 8 \, y_c^3 \, \log W - 8 \, y_c^3 \, \log 2 + 2 \, y_c^4 \right] +$$

$$\frac{\log(\log W + y_c)}{6 (\log 2)^2} \left((\log W)^2 + 4 \, \log W \, \log 2 + 3 \, (\log 2)^2 + 2 \, y_c \, \log W + \right.$$

$$\left. 4 \, y_c \, \log 2 + y_c^2 \right) (\log W + y_c)^2 - \frac{(-\log 2 + y_c)^2 \, \log(-\log 2 + y_c)}{2} +$$

$$\frac{(\log 2 + y_c)^2 \, \log(\log 2 + y_c)}{2} -$$

$$\left. \frac{(\log W + \log 2 + y_c)^4 \, \log(\log W + \log 2 + y_c)}{6 \, (\log 2)^2} \right\}$$

$$(A8)$$

References

[1] A. Giovannini and L. Van Hove, Z. Phys. C30 (1986) 391

[2] A. Giovannini and L. Van Hove, Acta Phys. Pol. B19 (1988) 495

[3] P. Abreu et al., DELPHI Collaboration, Z. Phys. C56 (1992) 63

[4] M. Arneodo et al., EMC Collaboration, Z. Phys. C35 (1987) 335

[5] G.J. Alner et al., UA5 Collaboration, Phys. Lett. B160 (1985) 193

[6] L. Van Hove and A. Giovannini, Acta Phys. Pol. B19 (1988) 917

[7] A. Giovannini, S. Lupia and R. Ugoccioni, Nucl. Phys. B (Proc. Suppl.) 25B (1992) 115

[8] F. Bianchi, A. Giovannini, S. Lupia and R. Ugoccioni, Z. Phys. C58 (1993) 71;
    F. Bianchi, A. Giovannini, S. Lupia and R. Ugoccioni, in Proceedings of the XXII International Symposium on Multiparticle Dynamics, (Santiago de Compostela, Spain, 1992), World Scientific, Singapore, 1993, p. 143

[9] G. Gustafson, Nucl. Phys. B392 (1993) 251;
    G. Gustafson and M. Olsson, Nucl. Phys. B406 (1993) 293

[10] W. Ochs, Z. Phys. C – Particles and Fields 23 (1984) 131;
     W. Ochs, J. Wosiek, Phys. Lett. B304 (1993) 144

[11] I.M. Dremin, R.C. Hwa, "Quark and gluon jets in QCD: factorial and cumulants moments", preprint OITS 531, December 1993

[12] Yu. L. Dokshitzer, Phys. Lett. B305 (1993) 295

[13] R. Ugoccioni and A. Giovannini, Z. Phys. C53 (1992) 239;
     A. Giovannini and R. Ugoccioni, invited talk, in: Fluctuations and Fractal Structure, Proceedings of the Ringberg Workshop on Multiparticle Production (Ringberg Castle, Germany, 1991), eds. R.C. Hwa, W. Ochs and N. Schmitz, World Scientific, Singapore, 1992, p. 264

[14] S. Lupia, A. Giovannini and R. Ugoccioni, Z. Phys. C59 (1993) 427

[15] Yu. L. Dokshitzer, V.A. Khoze, A.H. Mueller and S.I.Troyan, *Basics of Perturbative QCD*, Editions Frontières, Gif-Sur-Yvette, 1991

[16] R. Ugoccioni, A. Giovannini and S. Lupia, "The Generalized Simplified Parton Shower Model", DFTT 52/93, to be published in the Proceedings of the XXIII International Symposium on Multiparticle Dynamics, Aspen, CO, USA, 12-17 September 1993

Figure Captions

Fig. 1. The structure of the Simplified Parton Shower model (SPS) for parton production in virtuality Q and rapidity y. The degrading from the maximum allowed virtuality W is given by the product of eqs. (7) and (15). The splitting at (Q, y) is controlled by the product of eqs. (4), (10) and (14). Each dot represents a parton which further generates. Notice that here $Q_0 + Q_1 \leq Q$, $|y_0 - y| \leq \log \frac{Q}{Q_0}$.

Fig. 2. The structure of the Generalized Simplified Parton Shower model (GSPS) for clan production in virtuality Q and rapidity y. The production process is decoupled at each splitting both in virtuality and in rapidity (see eqs. (18) and (20)). Each blob represents a clan. Notice that here $Q_0 \leq Q$, $Q_1 \leq Q$, $|y_0 - y| \leq \log \frac{Q}{Q_0}$, $|y_1 - y| \leq \log \frac{Q}{Q_1}$.

Fig. 3. Diagrams for the probability that an ancestor, splitting at virtuality Q and rapidity y gets virtuality Q_0 and rapidity y_0 after emitting $N - 1$ clans, $r_N(Q_0 y_0 | Q y)$ (solid line); dashed diagrams correspond to the interchange of the final ancestor and the last produced clan, *i.e.*, to the probability to produce the $(N - 1)^{\text{th}}$ clan with virtuality Q_0 and rapidity y_0 from an ancestor splitting at virtuality Q and rapidity y, which can be described by the same $r_N(Q_0 y_0 | Q y)$.

Fig. 4. Diagrams for the probability that an ancestor of maximum allowed virtuality W gets virtuality Q_0 and rapidity y_0 after emitting $N - 1$ clans, $p_N(Q_0 y_0 | W)$ (solid line); dashed diagrams correspond to the interchange of the final ancestor and the last produced clan, *i.e.*, to the probability to produce the $(N - 1)^{\text{th}}$ clan with virtuality Q_0 and rapidity y_0 from an ancestor of maximum allowed virtuality W, which can be described by the same $p_N(Q_0 y_0 | W)$.

Fig. 5. Phase space domain in virtuality and rapidity for an ancestor parton of maximum allowed virtuality W. Dashed lines represent the approximation used for explicit calculations (eq. (78)). The thick solid line in the lowest right corner corresponds to the contribution of one-parton shower, *i.e.*, to the first diagram in Figure 4. In the central part of the figure we show the line corresponding to eq. (15).

Fig. 6. Clan density $p_\Sigma(y_0 | W)$ for one shower at $W = 50$ GeV (dotted line), 100 GeV (dashed line) and 500 GeV (solid line).

Fig. 7. Clan density $p_\Sigma(y_0 | W)$ resulting by the addition of two back-to-back showers at $W = 50$ GeV (dotted line), 100 GeV (dashed line) and 500 GeV (solid line).

Fig. 8. Average number of clans $\bar{N}(y_c, W)$ for a shower as a function of rapidity width y_c at $W = 50$ GeV (dotted line), 100 GeV (dashed line) and 500 GeV (solid line). The symbols represent the values of the average number of clans in full phase space.

Fig. 9. Normalized average number of clan $\pi^*(y_c^*, W)$ for a shower as a function of rescaled rapidity $y_c^* = y_c/y_{\text{fps}}$ at $W = 50$ GeV (dotted line), 100 GeV (dashed line) and 500 GeV (solid line).

Fig. 10. Phase space domain in virtuality and rapidity for an ancestor parton of maximum allowed virtuality W. Different domains defined in eq. (A1) are labelled by Roman letters; different integration domains of eq. (A6) are labelled by Greek letters.

Figure 1

$$\mathcal{P}(Q_0 Q_1 | Q) p(y_0 | Q_0 Q_1 Q y) \times$$

$$\delta[y_1 - y - \tanh^{-1}(\tfrac{B}{B+1}\tanh|y_0 - y|)]$$

n **final**

partons

$$p(Q|W)\delta(y - \tanh^{-1}\sqrt{1 - Q^2/W^2})$$

Q_{00}, y_{00}

Q_0, y_0

Q_{01}, y_{01}

Q, y

W

Q_1, y_1

$R_n(Q, y)$

$P_n(W)$

Figure 2

$$p(Q_0|Q)p(Q_1|Q)\times$$
$$p(y_0|Q_0Qy)p(y_1|Q_1Qy)$$

N **final**

clans

$$p(Q|W)\delta(y - \tanh^{-1}\sqrt{1 - Q^2/W^2})$$

Q_{00}, y_{00}

Q_0, y_0

Q_{01}, y_{01}

Q, y

Q_1, y_1

W

$r_N(Q, y)$

$p_N(W)$

Figure 3

Q

Q_0

y

y_0

Q_1, y_1

$\cdots$

Q

Q_0

y

y_0

Q_1, y_1

$\cdots$

$N = 2$

$N = 3$

Figure 4

W

Q,y

Q,y

Q_1,y_1

. . .

Q_0

y_0

y_0

W

Q,y

Q,y

Q_1,y_1

. . .

Q_0

y_0

y_0
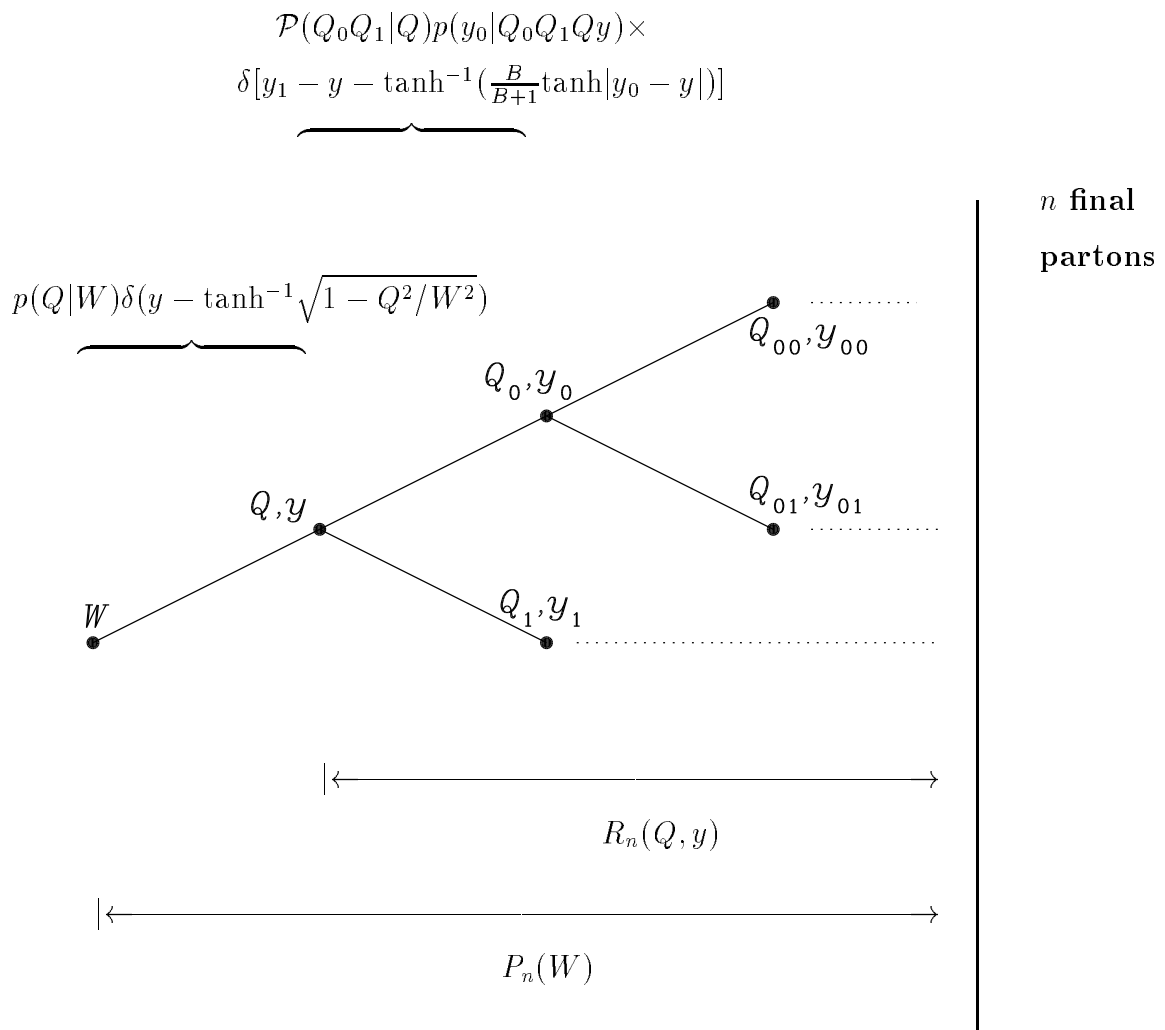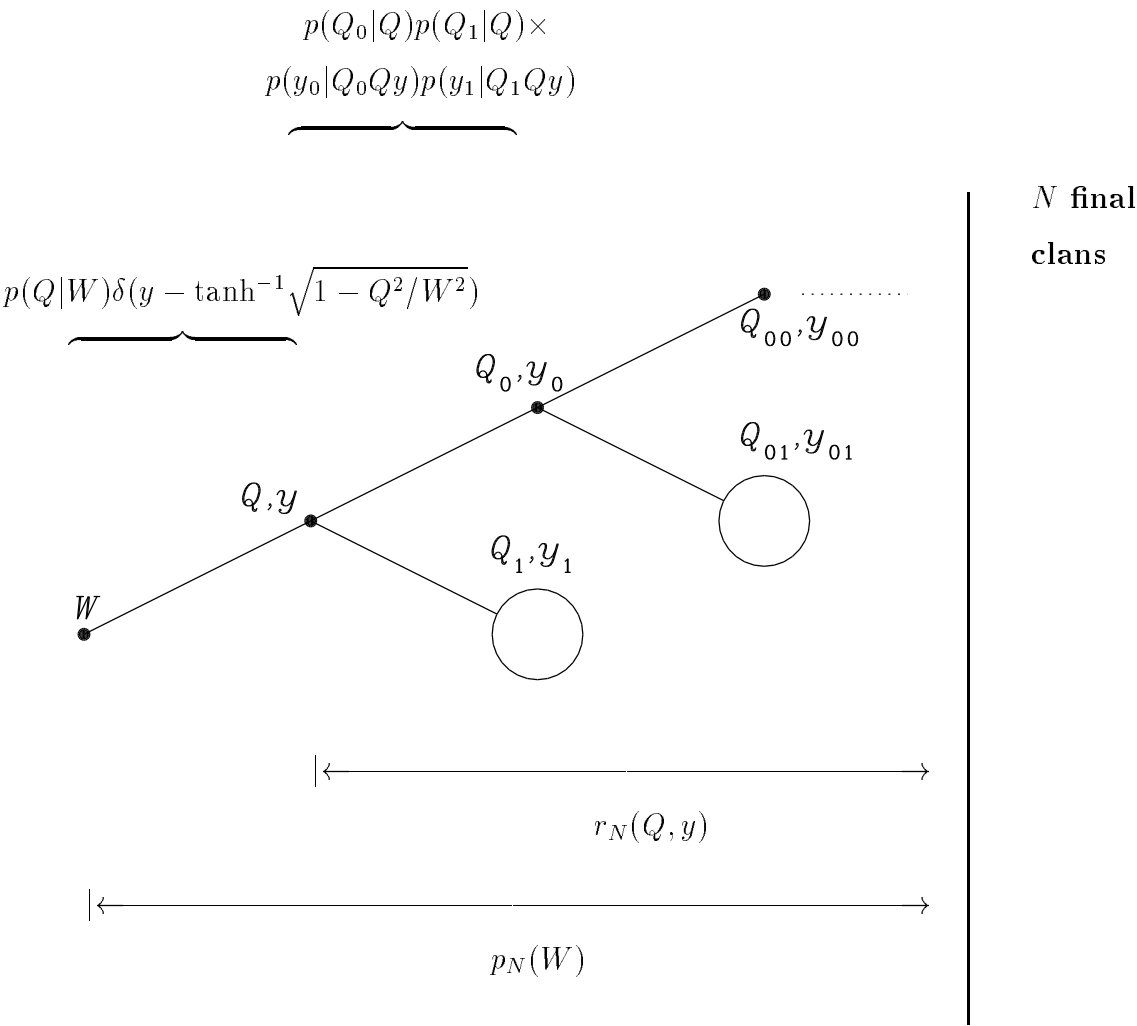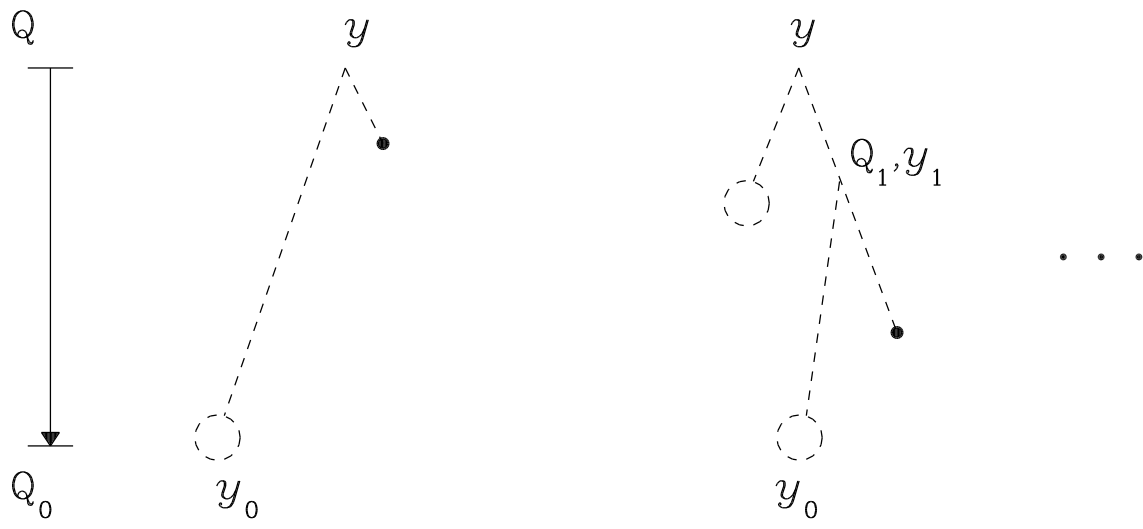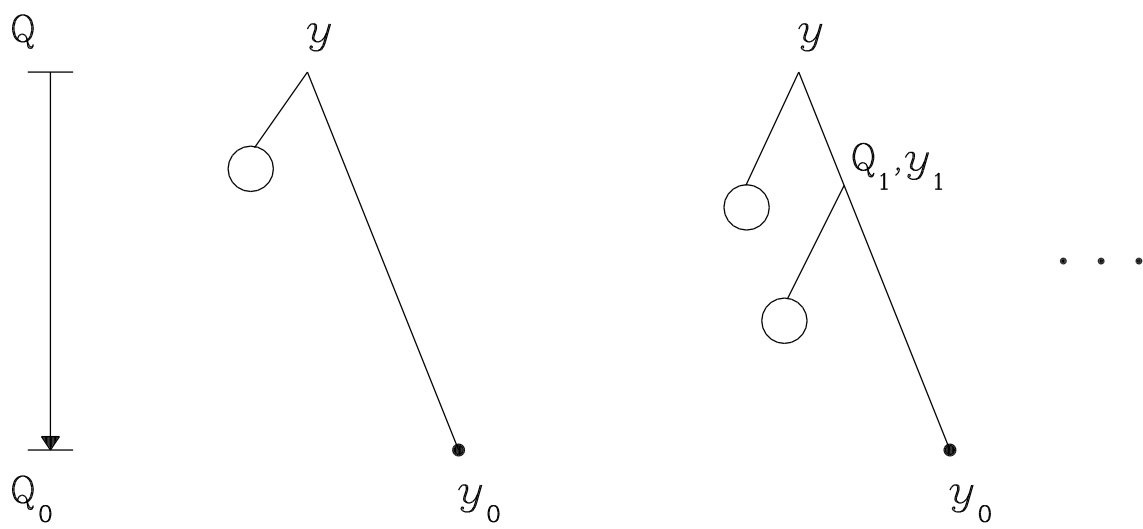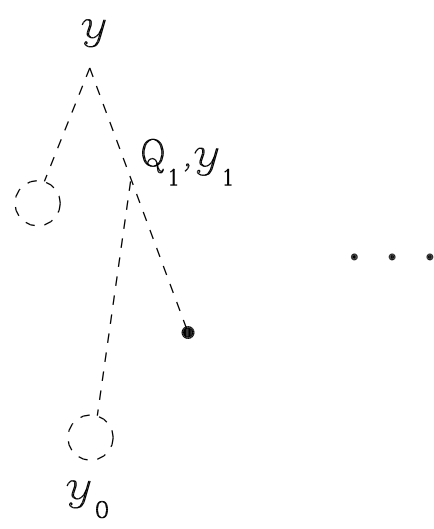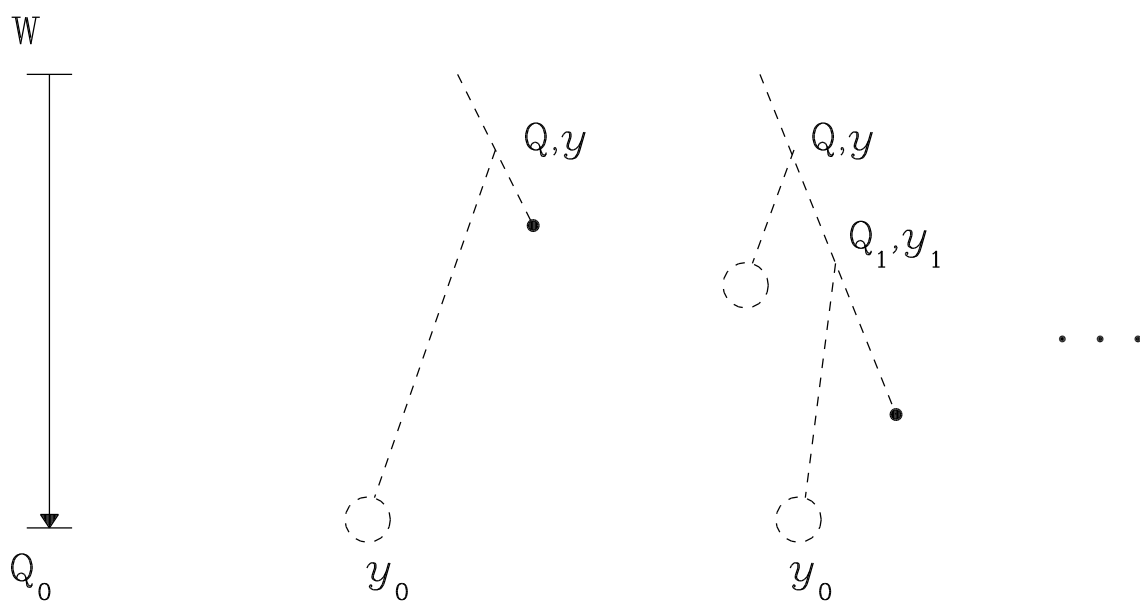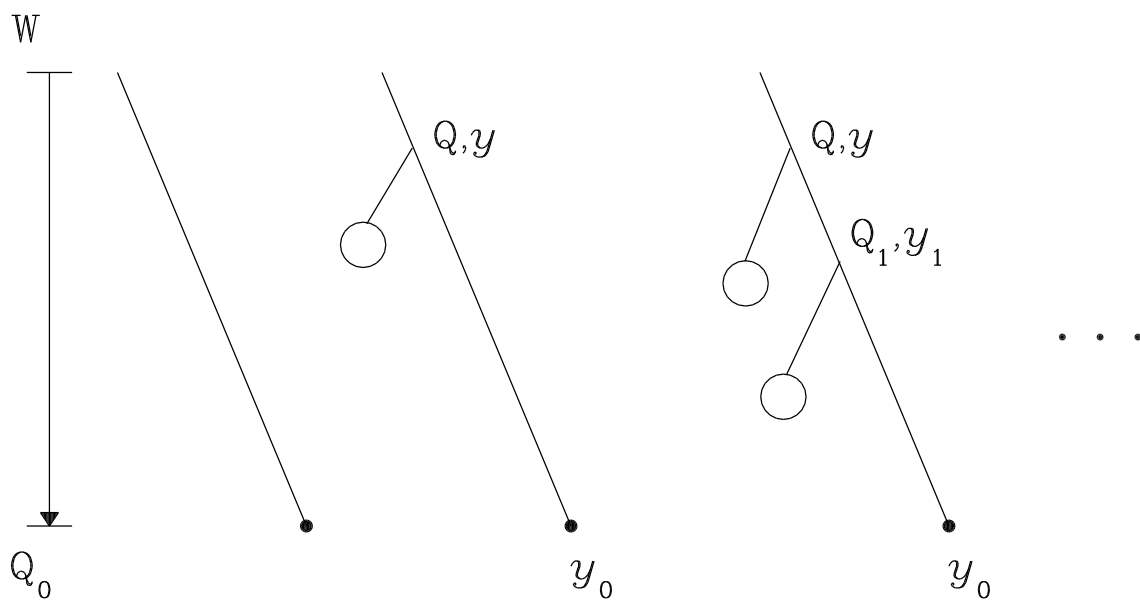
N = 1

N = 2

N = 3
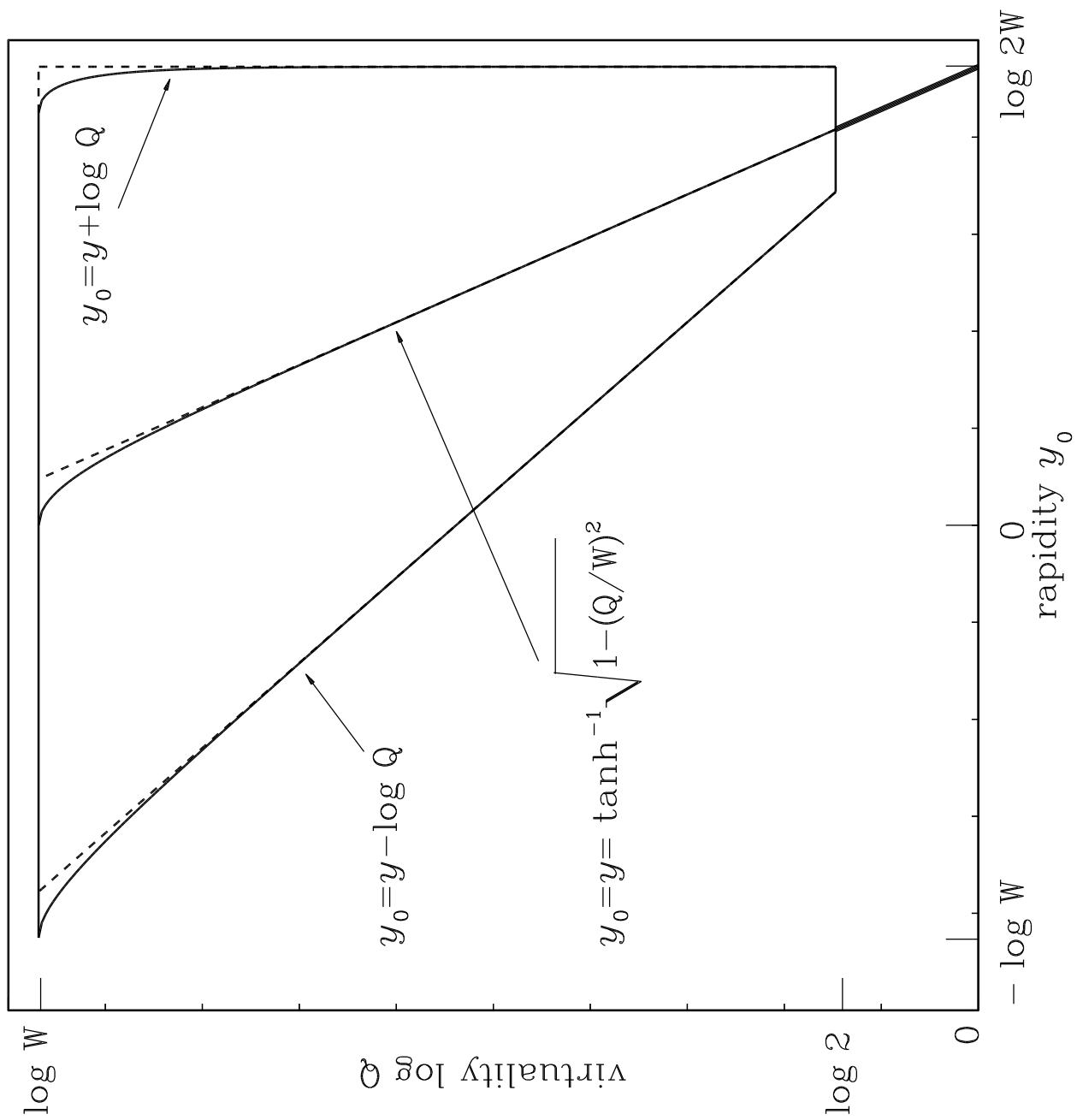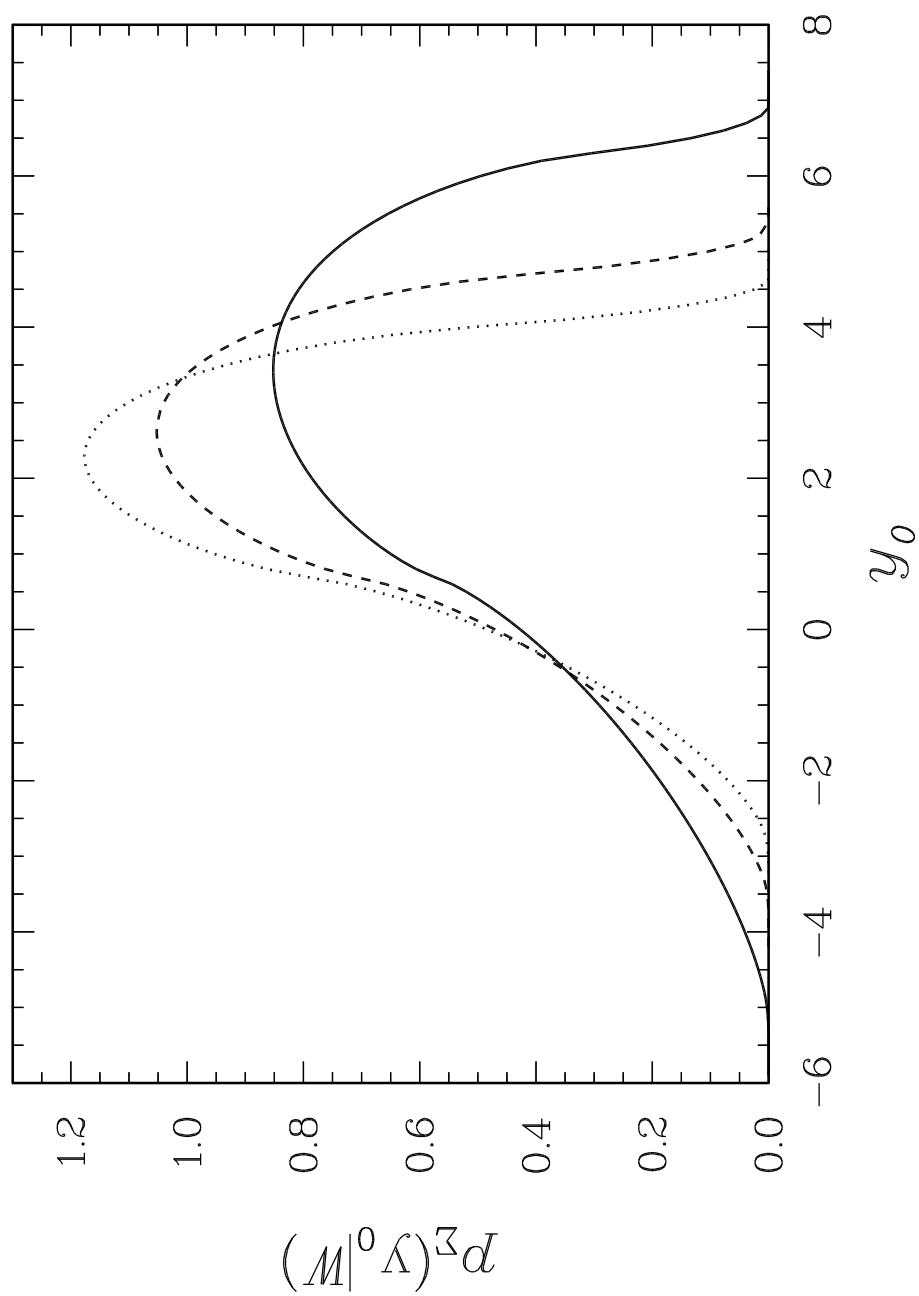
Figure 5

Figure 6

Figure 7
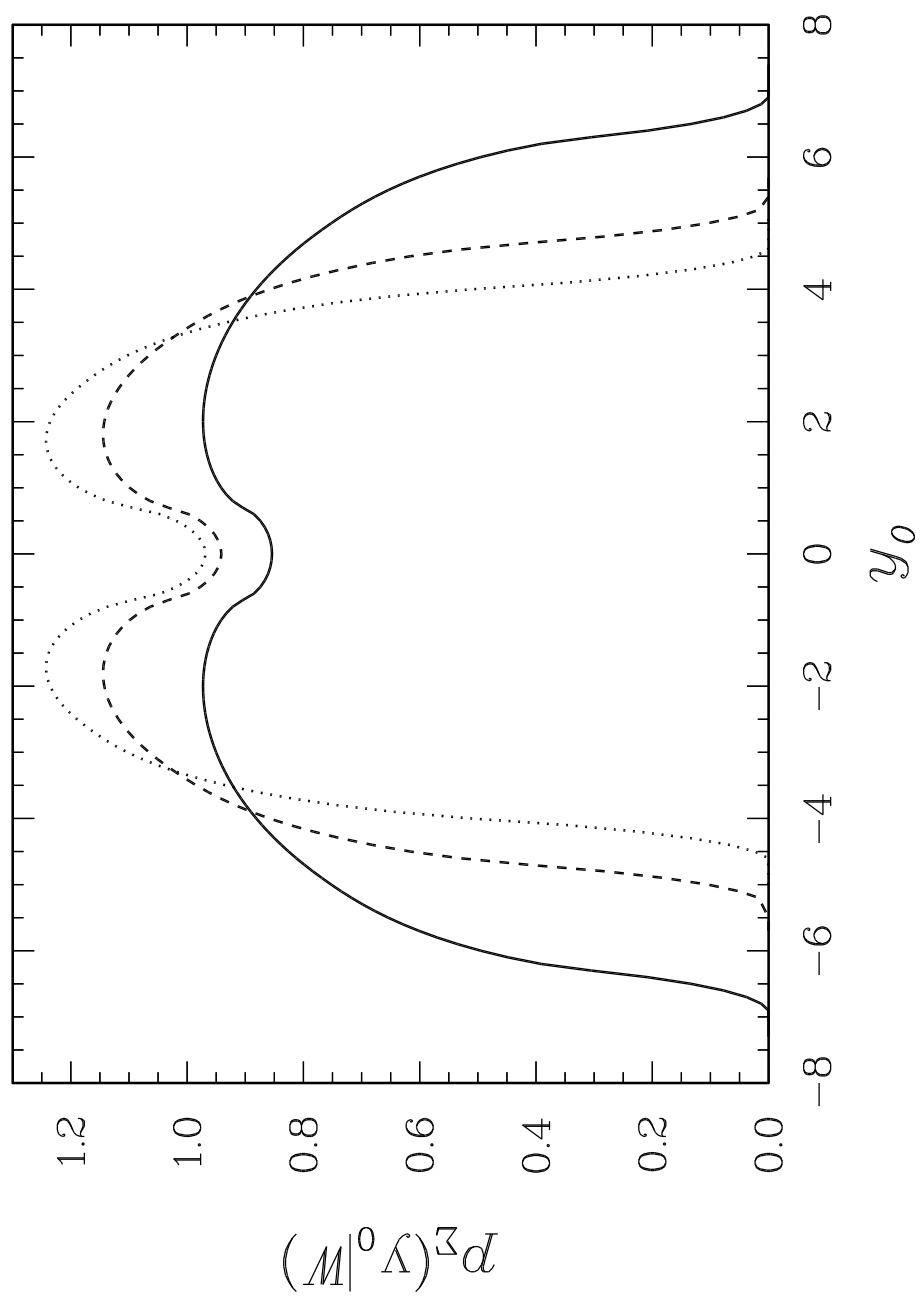
Figure 8
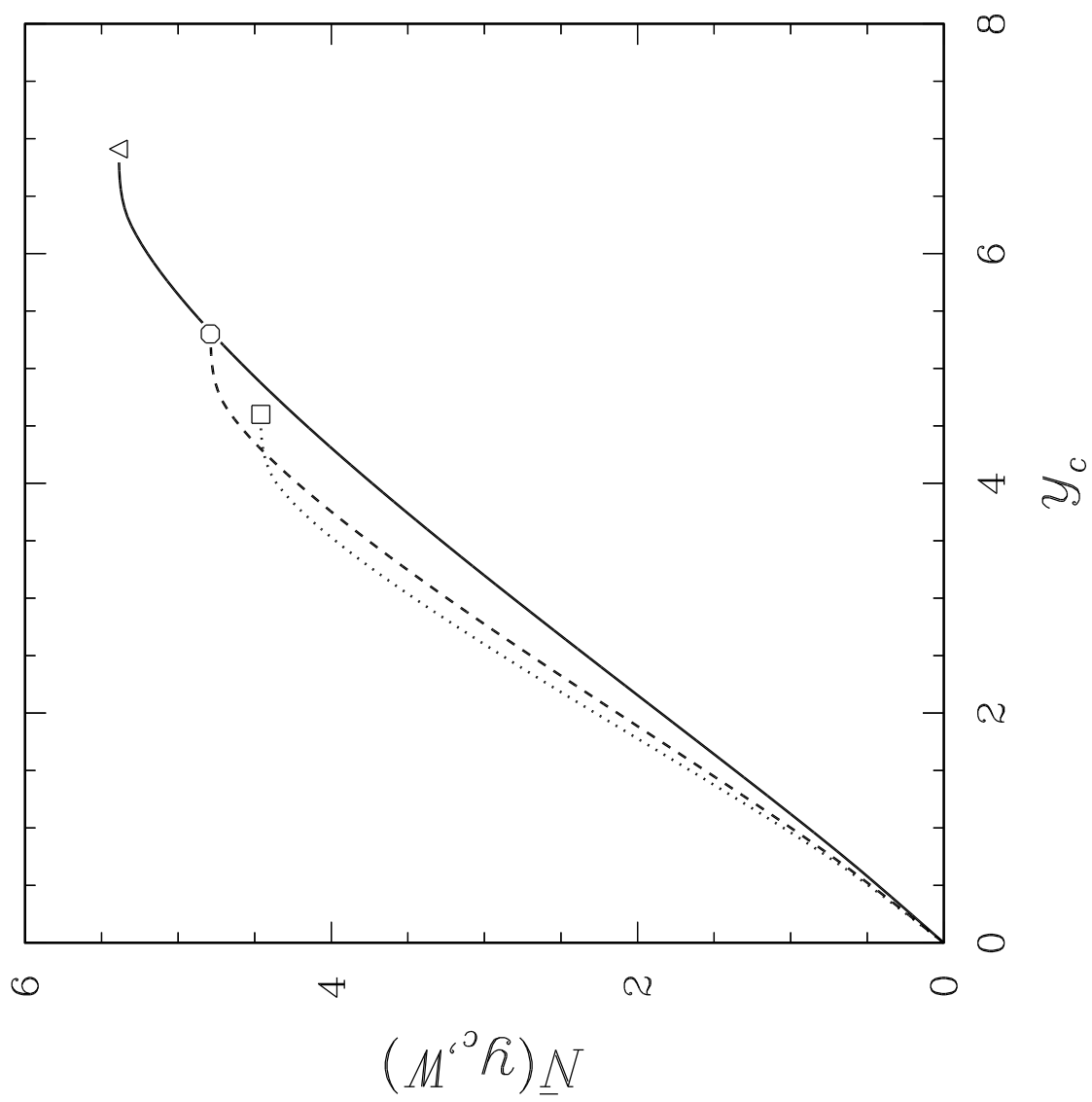
Figure 9
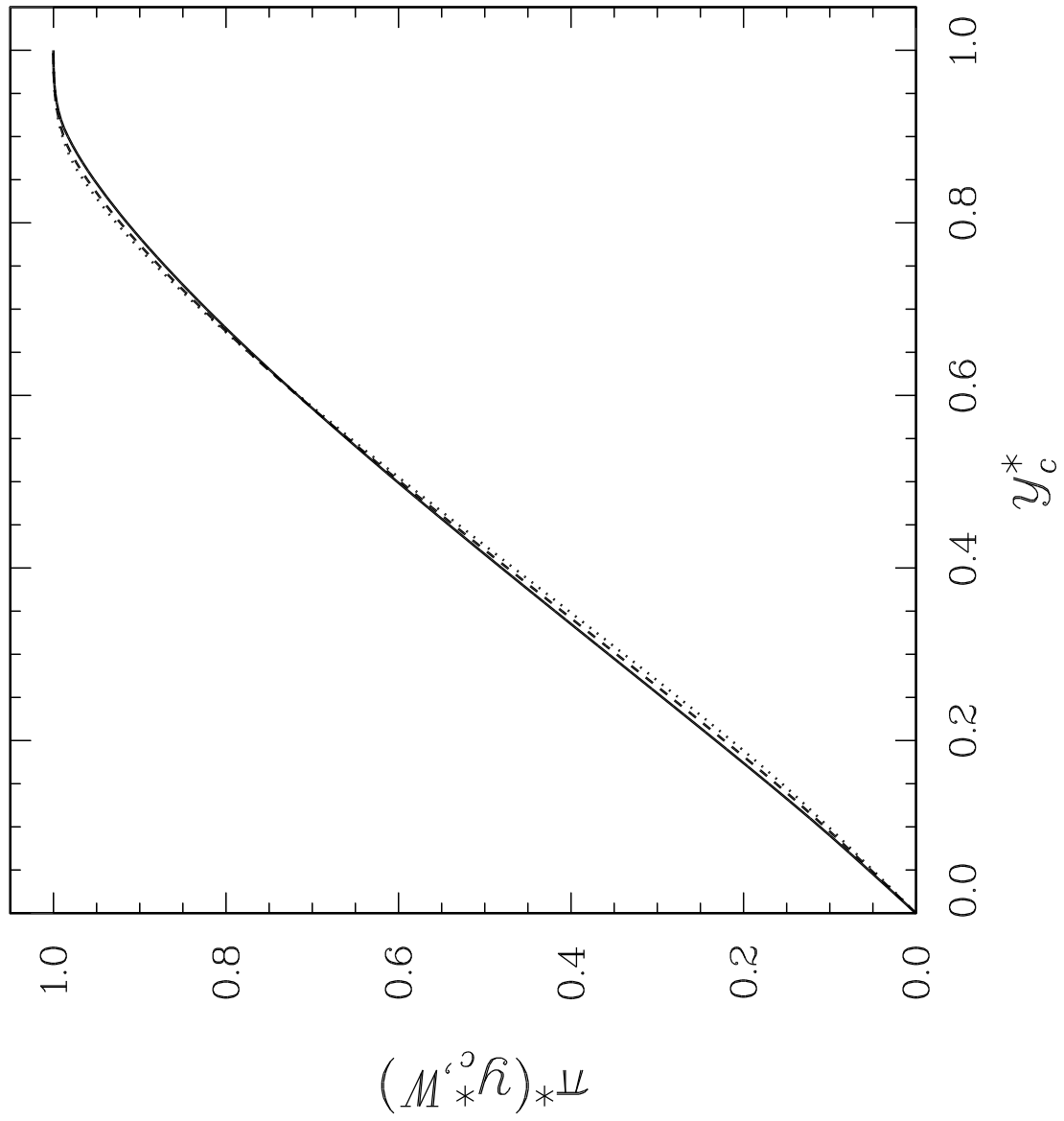
Figure 10
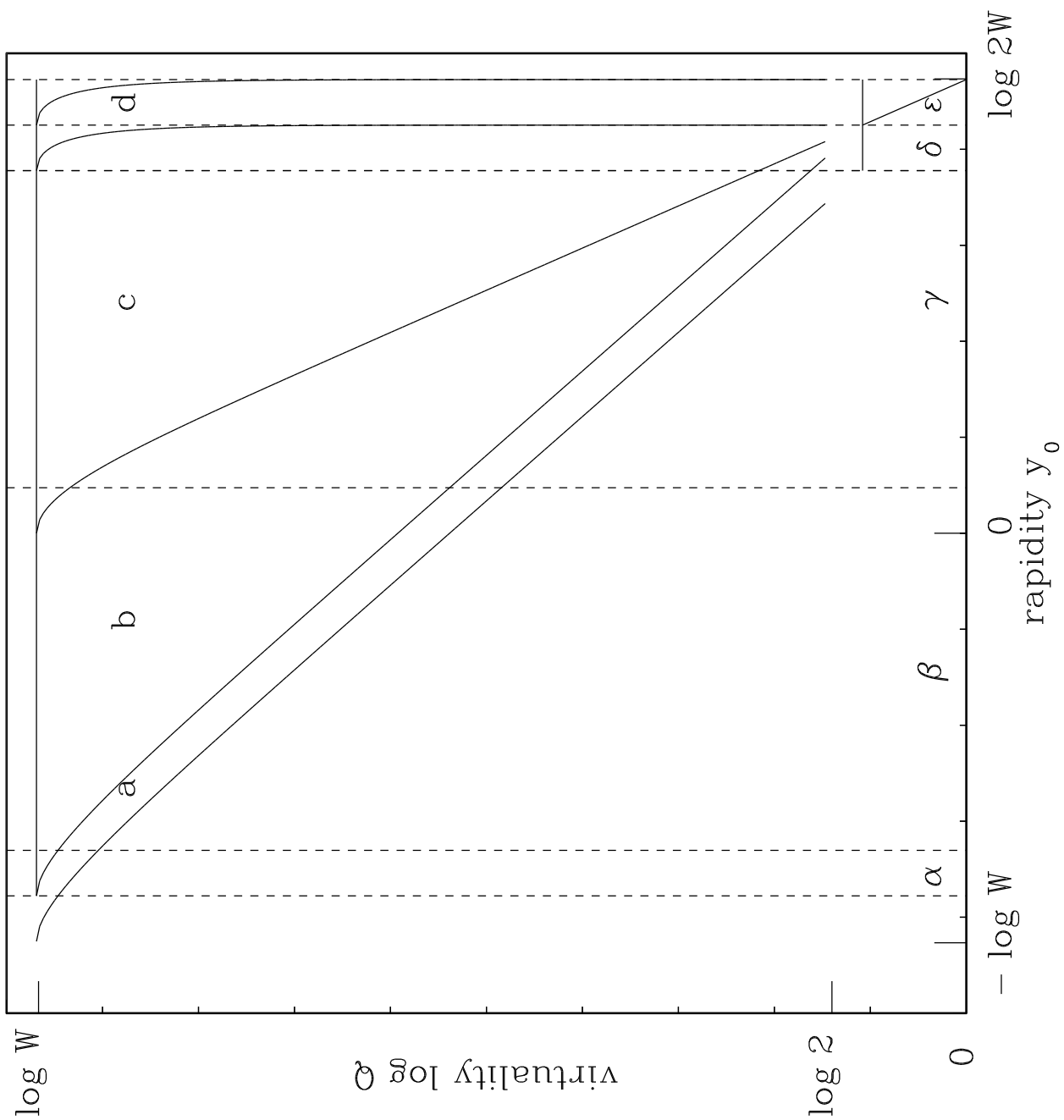
This figure "fig1-1.png" is available in "png" format from:

http://arXiv.org/ps/hep-ph/9404202v1

This figure "fig1-2.png" is available in "png" format from:

http://arXiv.org/ps/hep-ph/9404202v1

This figure "fig1-3.png" is available in "png" format from:

http://arXiv.org/ps/hep-ph/9404202v1

This figure "fig1-4.png" is available in "png" format from:

http://arXiv.org/ps/hep-ph/9404202v1

This figure "fig1-5.png" is available in "png" format from:

http://arXiv.org/ps/hep-ph/9404202v1

This figure "fig1-6.png" is available in "png" format from:

http://arXiv.org/ps/hep-ph/9404202v1

This figure "fig1-7.png" is available in "png" format from:

http://arXiv.org/ps/hep-ph/9404202v1

This figure "fig1-8.png" is available in "png" format from:

http://arXiv.org/ps/hep-ph/9404202v1

This figure "fig1-9.png" is available in "png" format from:

http://arXiv.org/ps/hep-ph/9404202v1

This figure "fig1-10.png" is available in "png" format from:

http://arXiv.org/ps/hep-ph/9404202v1